Involvement of Inducible Costimulator-B7 Homologous Protein Costimulatory Pathway in Murine Lupus Nephritis[1]

Hideyuki Iwai,[2*†] Masaaki Abe,[§] Sachiko Hirose,[§] Fumihiko Tsushima,[*] Katsunari Tezuka,[‡] Hisaya Akiba,[¶] Hideo Yagita,[¶] Ko Okumura,[¶] Hitoshi Kohsaka,[†] Nobuyuki Miyasaka,[†] and Miyuki Azuma[*]

Inducible costimulator (ICOS)-B7 homologous protein (B7h) is a new member of the CD28-B7 family of costimulatory molecules that regulates T cell-dependent humoral immune responses. In this study, we examined the involvement of this costimulatory pathway in the development and progression of lupus in NZB/W F_1 mice. Expression of ICOS on T cells was enhanced with disease progression, whereas B7h expression on B cells was down-regulated. Administration of anti-B7h mAb before the onset of renal disease significantly delayed the onset of proteinuria and prolonged survival. Blockade of B7h effectively inhibited all subclasses of IgG autoantibody production and accumulation of both Th1 and Th2 cells. Hypercellularity and deposition of IgG and C3 in glomeruli were significantly reduced. B7h blockade after the onset of proteinuria prevented the disease progression and improved the renal pathology. Our results demonstrated the involvement of the ICOS-B7h costimulatory pathway in the pathogenesis of lupus nephritis, and the blockade of this pathway may be beneficial for the treatment of human systemic lupus erythematosus. ***The Journal of Immunology,*** **2003, 171: 2848–2854.**

Systemic lupus erythematosus (SLE)[3] is a prototypic systemic autoimmune disease. SLE is characterized by dysregulated activation of both T and B cells, leading to generation of autoantibodies, particularly to dsDNA, that are critically involved in tissue damage (1, 2). The characteristic deposition of IgG in the kidney and other organs implies the involvement of IgG autoantibodies in the pathogenesis of SLE. NZB × NZW (NZB/W) F_1 mice develop a spontaneous autoimmune disease characterized by production of IgG antinuclear Abs, accumulation of immune complexes, and subsequent development of a fatal glomerulonephritis, which are reminiscent of human SLE (3). In both human SLE and the murine model of lupus nephritis, it has been shown that activation of autoantibody-producing B cells is dependent on T cell help through cytokines and costimulatory molecules (4). Recent reports demonstrated that the anergic state of autoreactive B cells is reversed by $CD4^+$ T cell help and regulated by T cell-mediated suppression (5). In the cognate interactions between T and B cells, both CD28-CD80/CD86 and CD154-CD40 are crucial costimulatory pathways for initial immune responses (6). Engagement of TCR by Ags presented by B cells rapidly induces CD154 expression on T cells, and its binding to CD40 on B cells promotes germinal center formation, B cell proliferation and differentiation, and isotype switching (7). The engagement of CD40 also induces CD80 and CD86 expression on B cells, and ligation of CD28 on T cells by the binding of CD80 and CD86 induces a strong costimulatory signal that promotes T cell activation and survival (8). Blockade of CD28 and/or CD40 pathways could inhibit the onset of murine lupus nephritis (9–13), suggesting the importance of both costimulatory pathways.

In addition to these pathways, other receptor/ligand pairs that are also involved in the T-B cognate interactions and may influence the pathogenesis of systemic autoimmune diseases include CD134-CD134 ligand (14), BAFF-BAFF ligands (15), and inducible costimulator (ICOS)-ICOS ligand (16, 17). ICOS is induced on T cells after activation (18). Its ligand B7 homologous protein (B7h) (19)/B7-related protein-1 (20)/GL50 (21)/ligand of ICOS (22) (hereafter designated B7h) is constitutively expressed on B cells and inducible on monocytes and dendritic cells at low levels (23). In addition to the expression on professional APCs, B7h is also inducible on fibroblasts (19) and endothelial cells (24) by proinflammatory cytokines such as IFN-γ and TNF-α. Ligation of ICOS strongly enhances the production of IL-4, IL-5, IFN-γ, and IL-10, but not IL-2 (18, 25, 26), suggesting a distinct costimulatory effect from CD28. IL-4 production by T cells was extremely impaired in the absence of ICOS (27). ICOS knockout mice exhibit profound defects in Th cell-dependent B cell responses, germinal center formation, and Ig class switching (28, 29). This deficit could be overcome by CD40 stimulation, suggesting that ICOS promotes isotype switching by regulating the CD40-CD154 pathway (28). Although these studies have substantiated a pivotal role of the ICOS-B7h costimulatory pathway in regulating humoral immune responses, its contribution to autoantibody production has not been well characterized. To investigate the involvement of the ICOS-B7h costimulatory pathway in the development and progression of lupus nephritis, we have examined the effects of anti-ICOS or anti-B7h mAb administration in lupus-prone NZB/W F_1 mice.

Departments of [*]Molecular Immunology and [†]Bioregulatory Medicine and Rheumatology, Graduate School, Tokyo Medical and Dental University, Tokyo, Japan; [‡]Pharmaceutical Frontier Research Laboratories, JT, Inc., Kanagawa, Japan; and Departments of [§]Pathology and [¶]Immunology, Juntendo University School of Medicine, Tokyo, Japan

Received for publication December 18, 2002. Accepted for publication July 17, 2003.

The costs of publication of this article were defrayed in part by the payment of page charges. This article must therefore be hereby marked *advertisement* in accordance with 18 U.S.C. Section 1734 solely to indicate this fact.

[1] This work was supported in part by Grant-in-Aid for Scientific Research from the Ministry of Education, Culture, Sports, Science and Technology and from the Ministry of Health, Labor, and Welfare of Japan.

[2] Address correspondence and reprint requests to Dr. Hideyuki Iwai, Department of Molecular Immunology, Division of Oral Health Sciences, Graduate School, Tokyo Medical and Dental University, 1-5-45 Yushima, Bunkyo-ku, Tokyo 113-8549, Japan. E-mail address: iwi.rheu@tmd.ac.jp

[3] Abbreviations used in this paper: SLE, systemic lupus erythematosus; ICOS, inducible costimulator; B7h, B7 homologous protein; MFI, mean fluorescent intensity; LN, lymph node; PAS, periodic acid-Schiff.

0022-1767/03/$02.00

Materials and Methods

Mice and mAb treatment

NZB/W F_1 and C.B-17/*scid* (SCID) female mice were purchased from SLC (Shizuoka, Japan) and Charles River Breeding Laboratories (Kanagawa, Japan), respectively, and maintained in the animal facility at Tokyo Medical and Dental University. Mice transgenic for the $OVA_{324-339}$-specific and I-A^d-restricted DO11.10 TCR-$\alpha\beta$ on a $RAG2^{-/-}$ background were generously supplied by Dr. S. Koyasu (Keio University, Tokyo, Japan). All procedures were reviewed and approved by the Animal Care and Use Committee of the Tokyo Medical and Dental University. The anti-mouse B7h (HK5.3, rat IgG2a) (30) and ICOS (B10.5, rat IgG2a) (31) mAbs were generated as described previously. HK5.3 blocked the binding of mouse ICOS-Ig to mouse B7h transfectants (30), and both B10.5 and HK5.3 could efficiently inhibit the ICOS-B7h-mediated proliferative responses by $CD4^+$ T cells in vitro (Ref. 30; H. Iwai, unpublished observation). In the experiments to see the effect of mAb treatment on the development of lupus, 2-mo-old NZB/W F_1 females were randomly divided into three groups and treated with control reagents, anti-B7h mAb (200 μg/body), or anti-ICOS mAb (100 μg/body) i.p. twice per week for 19 wk as described previously (10). Optimal doses for anti-B7h and anti-ICOS mAbs were determined according to our previous studies (10, 30). As the control reagents, PBS or rat IgG (200 μg/body; Sigma-Aldrich, St. Louis, MO) was used. As we observed similar results between the mice treated with PBS or rat IgG in all experiments, the results from the mice treated with PBS and rat IgG were combined and presented as a control group. In the experiments to see therapeutic effects, a cohort of NZB/W F_1 female mice was monitored for proteinuria every week from 5 mo of age. The treatment was started after observation of two consecutive proteinuria of >100 mg/dl. Three groups of mice received control reagent, anti-B7h mAb (200 μg/body), or anti-ICOS mAb (100 μg/body) i.p. three times per week until death or up to 12 mo of age.

Assessment of nephritis

For monitoring the development of nephritis, proteinuria was measured every week as described previously (32). Protein concentrations of >100 mg/dl of urine were considered positive. For histological evaluation of renal disease, mice were sacrificed at 7 mo of age or at 3 mo after the initial treatment. Kidneys were either fixed in formalin or snap-frozen in Tissue Tek (Sakura Finetechnical, Tokyo, Japan) for cryostat sectioning. Formalin-fixed tissue was embedded in paraffin, sectioned, and stained by the periodic acid-Schiff (PAS) method. The cellularity of 12 randomly selected glomeruli in each kidney cross-section was counted, and the severity of change was scored from 0 to 3 as follows: grade 0, normal (35–40 cells/glomerulus); grade 1, mild (41–50 cells/glomerulus); grade 2, moderate (51–60 cells/glomerulus); grade 3, severe (>60 cells/glomerulus) as described (33).

Frozen sections were fixed in acetone and 1% paraformaldehyde, and stained with FITC-conjugated anti-mouse IgG Ab (ICN/Cappel, Aurora, OH) or C3 Ab (ICN/Cappel), and propidium iodide (Sigma-Aldrich). The staining profiles were obtained with a fluorescence microscope (BX-50; Olympus, Tokyo, Japan) equipped with a charge-coupled device camera (PXL system; Photometrics, Tucson, AZ), and the image was analyzed by using IPLab Spectrum software (Signal Analytics, Vienna, VA). The quantitative evaluation of immunofluorescence was performed as described previously (34). The mean fluorescent intensity (MFI) of 15 glomeruli from each section was averaged.

ELISA of serum anti-dsDNA Ab

Serum samples were collected at 3, 5, and 7 mo of age, and the levels of anti-dsDNA total IgG, IgG1, IgG2a, and IgG2b Abs were measured by ELISA as described previously (35). A pooled serum from 7-mo-old NZB/W F_1 mice with severe nephritis was used as a standard. The titer of the standard serum was defined as 1 U, and the levels in individual samples are expressed as unit values.

mAbs and flow cytometry

mAbs against the following Ags were used for immunofluorescence analysis: CD3 (145-2C11, hamster IgG), CD4 (RM4-5, rat IgG2a), CD5 (53-7.3, rat IgG2a), CD8 (53-6.7, rat IgG2a), CD69 (H1.2F3, hamster IgG), CD25 (PC61, rat IgG1), CD45R/B220 (RA3-6B2, rat IgG2a), B7h (HK5.3), ICOS (B10.5), IFN-γ (XMG1.2, rat IgG1), IL-4 (BVD4-1D11, rat IgG2b), and IL-10 (JES5-16E3, rat IgG2b). All FITC-, PE-, or PerCP-conjugated mAbs and control Ig were obtained from BD Biosciences (San Diego, CA). Biotinylated anti-B7h and anti-ICOS mAbs were prepared in our laboratory and detected by PE-streptavidin (BD Biosciences). Multicolor staining for intracellular cytokine and cell surface Ags was performed as described previously (36). Immunofluorescence, flow cytometry, and data analysis were performed using FACSCalibur and CellQuest software (BD Biosciences).

Adoptive transfer experiments using DO11.10 TCR-transgenic T cells

To investigate the effect of in vivo treatment with anti-ICOS mAb on Ag-specific T cell responses, we performed the adoptive transfer of OVA-specific T cells from DO11.10 TCR-transgenic mice (37, 38). SCID (8-wk-old female) mice received a mixture of splenocytes and lymph node (LN) cells containing 3×10^6 of $CD4^+KJ1\text{-}26^+$ T cells from $RAG2^{-/-}$ DO11.10 mice. After 24 h, 1 mg of chicken OVA (grade V; Sigma-Aldrich) in IFA (Difco, Detroit, MI) was injected s.c. One hundred micrograms of control rat IgG or anti-ICOS mAb (B10.5) was administrated i.p. on days 0 and 2. Five days later, mice were sacrificed and the draining LNs were collected. Total LN cell numbers were counted, and the expansion and activation of OVA-specific T cells were examined using PE-conjugated anti-CD25 mAb and biotinylated anti-DO11.10 TCR (KJ1-26, mouse IgG2a; Caltag, Burlingame, CA) mAb, followed by allophycocyanin-streptavidin (BD Biosciences), or Annexin V^{FITC} (BD Biosciences) by flow cytometry. Alive cells, apoptotic cells, and large activated alive cells were determined to be annexin $V^-FSC^{medium\text{-}high}$, annexin V^+FSC^{low}, and annexin V^-FSC^{high} cells, respectively. Furthermore, isolated LN cells (5×10^5 cells/ml) were cultured in the presence of 2 μg/ml $OVA_{323-339}$ peptide (Bachem, Bubendorf, Switzerland), and cytokine production in the supernatants after 48-h culture was measured by ELISA. ELISA for IFN-γ, IL-4, and IL-10 was performed using ELISA kits (Ready-SET-Go; eBioscience, San Diego, CA) according to the protocols recommended by the manufacturer.

Statistical analysis

The log-rank and Mann-Whitney U tests were used. Values of $p < 0.05$ were considered significant.

Results

Expression of ICOS and B7h on splenocytes from NZB/W F_1 mice

We first examined the expression of ICOS and B7h on splenocytes from NZB/W F_1 mice before (at 2 mo of age) and after (at 7 mo of age) the onset of disease. A considerable percentage of T cells expressed ICOS in the splenocytes from NZB/W F_1 mice at 2 mo of age (Fig. 1). The expression of ICOS on T cells was gradually up-regulated as the age increased, and most T cells expressed ICOS at 7 mo of age in NZB/W F_1 mice. Similar results were obtained with PBLs (data not shown). Consistent with a previous observation (25), most B cells constitutively expressed B7h at all time points analyzed. Interestingly, the MFI was significantly ($p < 0.03$) decreased at 7 mo of age compared with 2 mo of age. These results prompted us to investigate the involvement of ICOS-B7h interactions in the development of lupus nephritis.

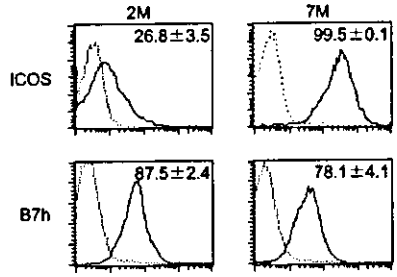

FIGURE 1. Expression of ICOS and B7h on splenocytes in NZB/W F_1 mice. Splenocytes from 2- and 7-mo-old NZB/W F_1 mice were stained with biotinylated anti-ICOS or anti-B7h mAb and FITC-labeled anti-CD3 or anti-CD45R mAb or with the appropriate fluorochrome-conjugated control Ig, followed by PE-streptavidin. Staining was analyzed by flow cytometry. An electronic gate was set on $CD3^+$ T cells or $CD45R^+$ B cells, and the expression of ICOS on T cells and B7h on B cells are represented as solid line with the control Ig staining as a dotted line. The values of mean percentages (ICOS) and MFI (B7h) ± SEM are indicated in the *upper right*. Data are representative of three separate experiments.

Administration of anti-B7h mAb before the onset of disease prevents the development of lupus

We examined the effects of anti-B7h or anti-ICOS mAb administration before the onset of lupus nephritis. We started the treatments from 2 mo of age when an obvious renal disease was not observed. At the cessation of treatment (6.5 mo of age), about one-half of the mice treated with control reagents or anti-ICOS mAb developed renal disease (proteinuria, >100 mg/dl), but none of the anti-B7h mAb-treated mice developed the disease (Fig. 2*A*). Although the mice treated with anti-B7h mAb eventually developed proteinuria after the cessation of treatment, the disease course was significantly ($p = 0.08$) different from that of the control group (Fig. 2*A*). The final survival rate of the anti-B7h mAb-treated mice at 10 mo of age was 80%, whereas all of the mice treated with control reagents or anti-ICOS mAb died of severe nephritis until this time point (Fig. 2*B*). The improvement of nephritis by the anti-B7h mAb treatment was verified by histological examination. Renal tissue sections from the control or anti-B7h mAb-treated mice at 7 mo of age were examined for the glomerular hypercellularity and the deposition of IgG and C3. The sections from the control mice showed a severe change including membranoproliferative changes and sclerosis of glomeruli (Fig. 3*Aa*), whereas these manifestations were not observed in the anti-B7h mAb-treated mice (*Ab*). Deposition of IgG (Fig. 3*A*, *c* and *d*) and C3 (not shown) to glomeruli was obvious in the control mice, but this was clearly inhibited in the anti-B7h mAb-treated mice. In the quantitative analyses, the anti-B7h mAb treatment showed a significant inhibition in the hypercellularity and the IgG and C3 deposition in glomeruli (Fig. 3*B*). These results indicated that the treatment with anti-B7h mAb before the onset of disease prevented the development of nephritis, although this preventive effect was lost upon cessation of the treatment.

Inhibition of anti-dsDNA IgG1, IgG2a, and IgG2b Ab production by anti-B7h mAb treatment

Consistent with our previous observation (10), the production of anti-dsDNA IgG Abs, including IgG1, IgG2a, and IgG2b subclasses, was first detectable in the control mice at 5 mo of age and became prominent at 7 mo of age (Fig. 4). All of these isotypes of Ab production were significantly suppressed in the mice treated with anti-B7h mAb. These results suggested that the anti-B7h mAb treatment inhibited both Th1- and Th2-mediated autoantibody production. In contrast, the treatment with anti-ICOS mAb did not consistently inhibit the production of anti-dsDNA Ab. The evaluation of respective IgG subclasses revealed that IgG1 was rather enhanced in the mice treated with anti-ICOS mAb at 3, 5, and 7 mo of age, whereas IgG2a and IgG2b were significantly inhibited. These results suggested a differential effect of the anti-ICOS mAb treatment on Th1- vs Th2-mediated immune responses.

We have monitored the serum Ab against the respective administrated rat IgGs. We failed to detect a substantial serum Ab against the anti-B7h rat IgG2a in the mice treated with anti-B7h mAb, whereas we observed a slight increase of Abs against the administrated control rat IgG and the anti-ICOS rat IgG2a in the control IgG- and anti-ICOS mAb-treated mice, respectively (data not shown). These results suggest an efficient inhibition of the anti-rat host responses by the treatment with anti-B7h mAb.

Effect of anti-B7h or anti-ICOS mAb treatment on lymphocyte status

To examine the effects of anti-B7h or anti-ICOS mAb treatment on lymphocytes in circulation and secondary lymphoid organs, we examined the cell number and lymphocyte population in peripheral blood and spleen at 7 mo of age. Consistent with our previous observation that T lymphopenia was observed at this age of NZB/W F_1 mice (39, 40), the control NZB/W F_1 mice exhibited a reduction of T lymphocytes in peripheral blood (Tables I and II). In the anti-B7h mAb-treated mice, this T lymphopenia was significantly ameliorated. In addition, splenomegaly and a high CD4/CD8 ratio of splenic T cells were characteristic features at this age of NZB/W F_1 mice, and these features were not observed in the mice treated with anti-B7h mAb (Tables I and II). The treatment with anti-ICOS mAb did not clearly affect the lymphocyte count and phenotypes as compared with the control mice (not shown).

We next examined the effects of mAb treatment on activational state of T cells. The percentages of $CD69^+$ or $CD25^+$ cells within $CD3^+$ T cells in the control NZB/W F_1 mice were clearly increased compared with the same age of BALB/c mice (CD69, 13.0 ± 0.1%; CD25, 12.9 ± 0.3%), and this increase was significantly inhibited by the anti-B7h mAb treatment (Fig. 5). A clear effect was not observed in the mice treated with anti-ICOS mAb. In the control NZB/W F_1 mice, $CD4^+$ T cells expressing IFN-γ,

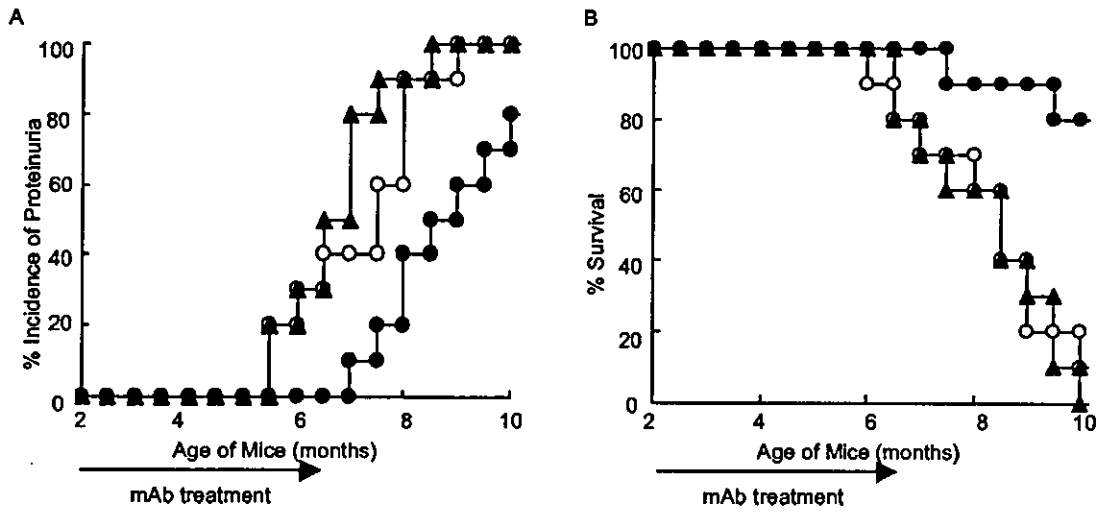

FIGURE 2. Effect of anti-B7h or anti-ICOS mAb treatment on the development of lupus nephritis. NZB/W F_1 female mice ($n = 10$ in each group) were treated with control reagents (○), anti-B7h mAb (●), or anti-ICOS mAb (▲) twice per week from 2 mo of age for 19 wk. Incidence of proteinuria (*A*) and survival rate (*B*) are shown. The data shown are representative of two independent experiments with similar results.

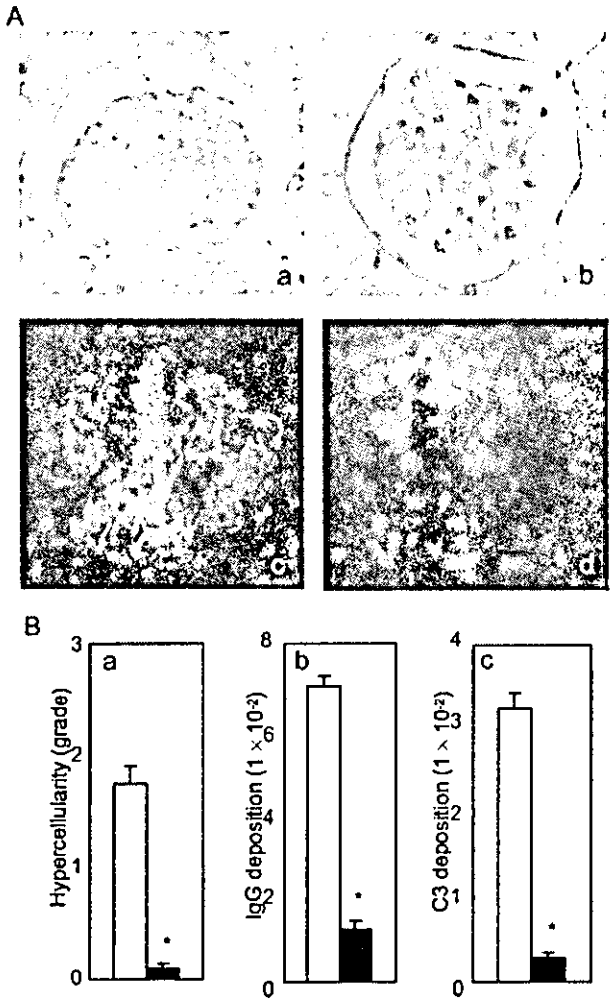

FIGURE 3. Evaluation of renal disease by histopathology. Kidney sections from the control reagents or anti-B7h mAb-treated mice at 7 mo of age were examined by PAS staining and immunofluorescence for IgG and C3 (green). Propidium iodide (red) was used for counterstain. *A*, Representative staining of PAS (*a* and *b*) and IgG deposition (*c* and *d*) from control reagent (*a* and *c*)- or anti-B7h mAb (*b* and *d*)-treated groups. Original magnification, ×100. *B*, Hypercellularity of glomeruli (*a*), and IgG (*b*) and C3 (*c*) deposition were quantitatively evaluated as described in *Materials and Methods*. The mean scores ± SEM of four mice in the control reagent-treated (□) or anti-B7h mAb (■)-treated group are shown. *, Statistically different ($p < 0.05$).

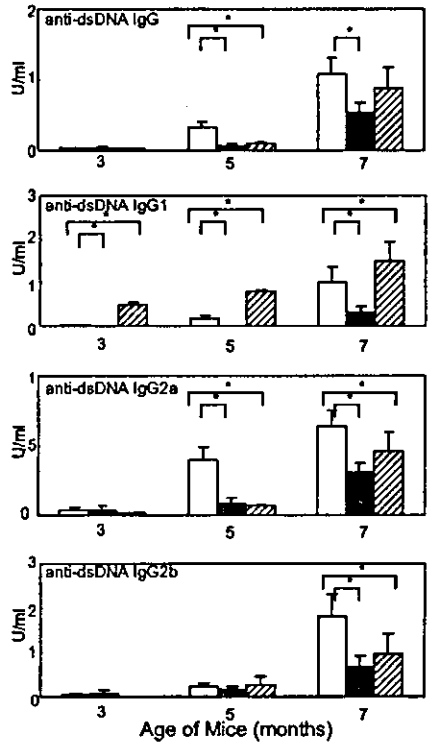

FIGURE 4. Effect of anti-B7h or anti-ICOS mAb treatment on serum anti-dsDNA IgG Ab. Serum samples from the control reagent (□)-, anti-B7h mAb (■)-, or anti-ICOS mAb (▨)-treated mice were obtained at 3, 5, and 7 mo of age. Serum levels of anti-dsDNA total IgG, IgG1, IgG2a, and IgG2b Abs were measured by ELISA. Data shown are the mean ± SEM of 10 mice from two independent experiments in each group. *, Statistically different ($p < 0.05$).

IL-4, and IL-10 were increased compared with those of the same age of BALB/c mice (IFN-γ, 0.8 ± 0.04%; IL-4, 0.4 ± 0.06%; IL-10, 0.2 ± 0.04%), which were significantly reduced by the anti-B7h mAb treatment. The treatment with anti-ICOS mAb showed less inhibitory effects on IFN-γ and IL-10, whereas no inhibition was observed on IL-4. $CD8^+$ T cells expressing IFN-γ, IL-4, and IL-10 in the control NZB/W F_1 mice were 0.5 ± 0.3%, 0.2 ± 0.1%, and 0.2 ± 0.1%, respectively, and these were not affected by the anti-B7h or anti-ICOS mAb treatment (data not shown). These results suggested that the anti-B7h mAb treatment inhibited the activation of both Th1 and Th2 cells, whereas the anti-ICOS mAb treatment had less inhibitory effect on T cell activation.

Therapeutic effect of anti-B7h mAb treatment after the onset of lupus nephritis

To investigate the effects of anti-B7h or anti-ICOS mAb treatment on ongoing lupus nephritis, we treated NZB/W F_1 mice that had developed renal disease (proteinuria, >100 mg/dl) three times per week up to 12 mo of age. The mice treated with either control reagents or anti-ICOS mAb exhibited no significant improvement in proteinuria (not shown) and in survival rate, and all mice died within 2 mo after the initial treatment (Fig. 6*A*). The treatment with

Table I. *Effects of anti-B7h mAb treatment on peripheral blood*[a]

	Total Lymphocytes ($\times 10^3/\mu l$)	T Cells ($\times 10^3/\mu l$)	Conventional B Cells ($\times 10^3/\mu l$)	$CD5^+$ B Cells ($\times 10^3/\mu l$)
Control reagents	6.6 ± 0.4	4.0 ± 0.4	1.2 ± 0.0	0.3 ± 0.0
Anti-B7h mAb	7.9 ± 0.2[b]	5.5 ± 0.3[b]	1.4 ± 0.1	0.6 ± 0.1[b]

[a] Absolute lymphocyte counts in peripheral blood from the mice at 7 mo of age were measured. Lymphocytes were stained with FITC-conjugated anti-CD45R mAb and PerCP-conjugated anti-CD3 mAb or PE-conjugated anti-CD5 mAb. $CD3^+$ $CD45R^-$, $CD5^-$ $CD45R^+$, and $CD5^+$ $CD45R^+$ cell counts are presented as T cells, conventional B cells, and $CD5^+$ B cells, respectively. Values are the means ± SEMs from each group ($n = 10$).

[b] Statistically different from the control reagent-treated group ($p < 0.05$)

Table II. *Effects of anti-B7h mAb treatment on splenocytes*[a]

	Total Lymphocytes ($\times 10^7$)	$CD4^+$ T Cells ($\times 10^7$)	$CD8^+$ T Cells ($\times 10^7$)	CD4/CD8
Control reagents	17.6 ± 1.9	5.4 ± 0.6	0.7 ± 0.1	8.0 ± 0.6
Anti-B7h mAb	8.0 ± 1.9[b]	2.8 ± 0.5[b]	0.8 ± 0.0[b]	3.5 ± 0.9[b]

[a] Splenocytes from a 7-mo-old individual mouse were counted, and cells were stained with FITC-conjugated anti-CD8 mAb, PE-conjugated anti-CD4 mAb, and PerCP-conjugated anti-CD3 mAb. $CD3^+$ $CD4^+$ $CD8^-$ and $CD3^+$ $CD4^-$ $CD8^+$ cell counts were presented as $CD4^+$ T and $CD8^+$ T cells, respectively. Values are the means ± SEMs from each group of four mice.
[b] Statistically different from the control reagent-treated group ($p < 0.05$).

anti-B7h mAb significantly ($p = 0.036$) improved the survival rate compared with the control group, and 40% of mice survived at 3 mo after the initiation of treatment. In several mice, the levels of proteinuria and anti-dsDNA Ab production were improved after the anti-B7h mAb treatment (data not shown). The improvement of renal disease by anti-B7h mAb treatment was verified by histological examination in the mice that survived by the anti-B7h mAb treatment. The hypercellularity and the deposition of IgG and C3 in glomeruli observed in the mice without treatment at 7 mo of age were clearly improved in the mice that survived at 12 mo of age from the anti-B7h mAb-treated group (Fig. 6*B*). These results suggest that the B7h blockade could ameliorate ongoing lupus nephritis and inhibit disease progression.

The effects of anti-ICOS mAb on OVA-specific T cell responses

In the above studies, we have observed a lower or reverse effect of anti-ICOS mAb treatment on autoantibody production and T cell activation. To see actual inhibitory or activating properties of anti-ICOS mAb, we investigated the effects of anti-ICOS mAb treatment in the adoptive transfer of OVA-specific T cells from $RAG2^{-/-}$ DO11.10 TCR-transgenic mice. Five days after the transfer of 3×10^6 KJ1-26^+ T cells and OVA immunization with IFA, there was a significant expansion of Ag-specific T cells in the draining LN from control rat IgG-treated mice ($2.6 \pm 0.1 \times 10^6$ cells) compared with the mice immunized with IFA alone ($0.02 \pm 0.05 \times 10^6$ cells). The anti-ICOS mAb-treated mice showed a lower number of KJ1-26^+ T cells ($1.9 \pm 0.3 \times 10^6$ cells) (Table III). Unexpectedly, flow-cytometric analysis revealed that the anti-ICOS mAb treatment significantly increased the percentage of apoptotic cells as well as the percentage of large activated cells defined by annexinV^-FSC^{high}. Furthermore, the anti-ICOS mAb treatment significantly increased the percentage of $CD25^+$ cells within KJ1-26^+ T cells. In addition, LN cells from the anti-ICOS mAb-treated SCID mice produced higher amounts of IFN-γ, IL-4, and IL-10 after stimulation with OVA peptide. These results indicate that the treatment with anti-ICOS mAb promoted Ag-specific T cell activation and apoptosis/activation induced cell death, suggesting an agonistic activity of the anti-ICOS mAb.

Discussion

An array of costimulatory molecules has been implicated in the pathogenesis of lupus nephritis in NZB/W F_1 mice (9–11, 14, 41). In this study, we first demonstrated a critical contribution of the ICOS-B7h pathway as well. The blockade of B7h by administration of anti-B7h mAb inhibited the onset and the progression of glomerulonephritis and prolonged the survival. The improvement in clinical manifestations was correlated with the inhibition of cellular and humoral immune responses mediated by both Th1 and Th2 cells and histopathological amelioration.

ICOS is expressed on naive T cells only after activation (18). Surprisingly, most T cells expressed ICOS at a high level, and considerable percentages of T cells expressed activation markers, CD69 and CD25, at 7 mo of age in NZB/W F_1 mice, suggesting aberrant activation of T cells with disease progression. In contrast to the inducible expression of ICOS on T cells, its ligand B7h is constitutively expressed on naive B cells (19, 23). A recent report demonstrated that B7h on B cells was extinguished after activation through surface Ig- and IL-4-mediated signaling, and a costimulation through CD40 was capable of restoring the surface expression of B7h (42). In NZB/W F_1 mice, we also observed the down-regulation of B7h on splenic B cells with disease progression (Fig.

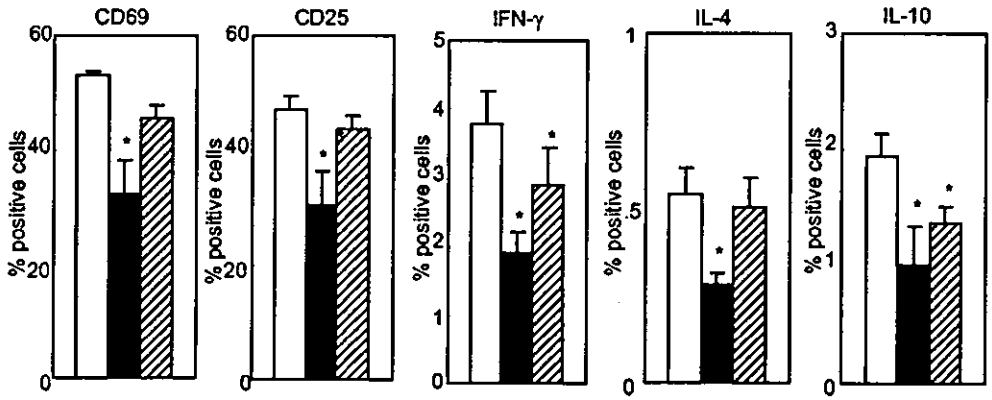

FIGURE 5. Expression of activation markers and cytokines in splenic T cells. Splenocytes from the control reagent (□)-, anti-B7h mAb (■)-, or anti-ICOS mAb (▨)-treated mice at 7 mo of age were obtained. Cells were stained with combinations of PE-conjugated anti-CD69 or anti-CD25 mAb and PerCP-conjugated anti-CD3 mAb, and PE-conjugated anti-IFN-γ, anti-IL-4, or anti-IL-10 mAb and PerCP-conjugated anti-CD4 mAb. An electronic gate was set on either $CD3^+$ or $CD4^+$ lymphocytes, and the percentages of $CD69^+$ or $CD25^+$ cells within $CD3^+$ T cells and the percentages of IFN-γ^+, IL-4^+ or IL-10^+ cells within $CD4^+$ T cells were analyzed by flow cytometry. Data represent the mean percentages ± SEM of four mice in each group. *, Statistically different from the control group ($p < 0.05$).

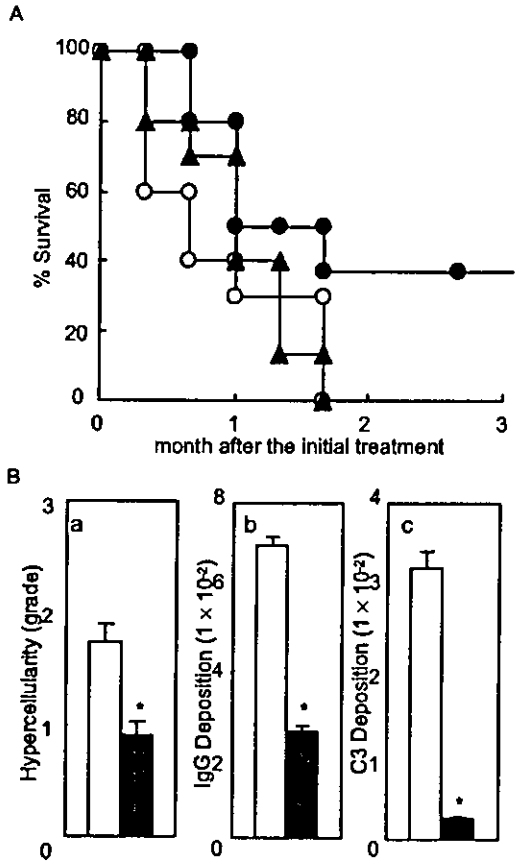

FIGURE 6. Effect of anti-B7h or anti-ICOS mAb treatment after the onset of nephritis. NZB/W F_1 mice (n = 10 in each group) with initial proteinuria (>100 mg/dl) were treated with control reagents (○), anti-B7h mAb (●), or anti-ICOS mAb (▲) three times per week until 12 mo of age. *A*, Survival rate after the initial treatment. *B*, Severity of nephritis evaluated by histological examination. Hypercellularity of glomeruli (*a*), and IgG (*b*) and C3 (*c*) deposition were quantitatively evaluated as described in *Materials and Methods*. Data represent the mean scores ± SEM of four mice at 7 mo of age with control reagents (□) and at 12 mo of age with anti-B7h mAb treatment (■). *, Statistically different ($p < 0.05$).

1). This might result from the cognate interaction with T cells during the process of disease progression.

In the present experiments, we have observed contradictory results between the anti-B7h and anti-ICOS mAb treatments. The treatment with anti-B7h mAb showed a consistent amelioration of both clinical and pathological manifestations, immunological abnormality including expression of T cell activation markers and cytokines, and all subclasses of anti-dsDNA autoantibody production. In contrast, the administration of anti-ICOS mAb failed to ameliorate clinical manifestations assessed by proteinuria and survival rate, although this treatment significantly inhibited IFN-γ and IL-10 production by splenic T cells and serum IgG2a and IgG2b anti-dsDNA Ab production. It should be noted that the anti-ICOS mAb treatment induced early production of IgG1 anti-dsDNA Ab, and this was further enhanced with age. In addition, this treatment did not significantly affect IL-4 production unlike the treatment with anti-B7h mAb. These results suggest that the anti-ICOS mAb treatment potentially has a reverse effect on Th2-mediated immune responses. In fact, the adoptive-transfer experiments using DO11.10 TCR-transgenic T cells demonstrated an agonistic property of the anti-ICOS mAb used in this study. In the $CD4^+$ T cell responses against OVA, the treatment with anti-ICOS mAb apparently promoted activation of both Th1 and Th2 cells and apoptosis. Previous reports using the same anti-ICOS mAb (B10.5) demonstrated the opposing effect of this mAb on acute vs chronic graft-vs-host disease (43), and the ameliorating effect on a chronic colitis induced by transfer of $CD4^+CD45RB^{high}$ T cells by enhancing Th2 cytokine production and apoptosis of infiltrating T cells (44). In addition, we also observed that treatment with various doses of anti-ICOS mAb (50, 100, 300 μg/body) persistently exacerbated the collagen-induced arthritis (H. Iwai and M. Azuma, unpublished observation), whereas the anti-B7h mAb treatment efficiently ameliorated the arthritis by inhibiting both Th1- and Th2-mediated immune responses (30). Taken together, it is likely that the binding of anti-ICOS mAb (B10.5) to T cells induced an agonistic signal to T cells, especially to Th2 cells in our NZB/W F_1 model. Preferential expression of ICOS on Th2 cells has been reported (45–47). Therefore, the differential expression of ICOS between Th1 and Th2 cells and the differential contribution of Th1 and Th2 cells to the development of lupus may result in different outcomes of the binding of anti-ICOS mAb in this model.

It has been shown that the ICOS-B7h costimulatory pathway is preferentially involved in the effector phase of immune responses rather than the induction phase (47, 48). We previously examined the effects of anti-CD80 and -CD86 mAbs on the development and progression of lupus nephritis in NZB/W F_1 mice with similar protocols (10). Based on the incidence of proteinuria and the survival rate at 10 mo of age, the inhibitory effect of the anti-B7h mAb treatment before the onset of disease seems to be inferior to

Table III. *Effects of anti-ICOS mAb treatment on the adoptive transfer of OVA-specific T cells*[a]

	KJ1-26⁺ T[b] (×10⁶ Cells)	Apoptotic/ Dead Cells[c] (%)	Alive Cells (%)	Activated Cells (%)	CD25⁺ Cells[d] (%)	Cytokine Production[e] IFN-γ (ng/ml)	IL-4 (pg/ml)	IL-10 (pg/ml)
Rat IgG	2.6 ± 0.1	12.7 ± 0.9	86.8 ± 0.9	12.5 ± 0.1	31.7 ± 1.2	50.3 ± 8.5	45 ± 7	767 ± 75
Anti-ICOS mAb	1.9 ± 0.3	28.1 ± 2.5[f]	71.3 ± 2.6[f]	17.9 ± 1.5[f]	40.6 ± 1.0[f]	63.1 ± 2.4	183 ± 66	906 ± 131

[a] SCID mice received 3 × 10^6 KJ1-26⁺ T cells from $RAG2^{-/-}$ DO11.10 TCR-transgenic mice and were immunized with 1 mg of OVA in IFA. Either 100 μg each of anti-ICOS mAb or control rat IgG was administrated i.p. on days 0 and 2. At day 5, total LN cell numbers were counted, and cells were stained with biotinylated anti-DO11.10 TCR mAb, followed by allophycocyanin-avidin and either FITC-conjugated anti-CD4 mAb, Annexin V^{FITC}, or PE-conjugated anti-CD25 mAb.

[b] The counts for KJ1-26⁺ cells were calculated from the total cell number of LN cells and the percentage of KJ1-26⁺ cells. More than 99% of KJ1-26⁺ cells were costained with anti-CD4 mAb.

[c] The percentages of annexin V^- $FSC^{medium-high}$, annexin V^+ FSC^{low}, and annexin V^- FSC^{high} cells in total LN cells are presented as alive cells, apoptotic/dead cells, and activated cells, respectively.

[d] The percentages of CD25⁺ cells within KJ1-26⁺ cells are shown.

[e] Production of IFN-γ, IL-4, and IL-10 in the supernatants from LN cell cultures in the presence of $OVA_{323-339}$ peptide for 48 hr was measured by ELISA. Data are representative of two separate experiments and expressed as the means ± SEMs from each group of three mice.

[f] Statistically different from the control rat IgG-treated group ($p < 0.05$).

that of the anti-CD80/86 mAb treatment. Nevertheless, the survival rate at 12 mo of age in the therapeutic treatment was comparable with that of the CD80/86 mAb treatment. Consistent with our recent results in a collagen-induced arthritis model (30), the B7h blockade consistently showed an effectiveness against ongoing autoimmune diseases.

In conclusion, the blockade of B7h prevented the onset and progression of lupus nephritis in NZB/W F_1 mice by efficiently inhibiting both cellular and humoral immune responses associated with disease. Our results demonstrated a critical role of the ICOS-B7h costimulatory pathway in the pathogenesis of lupus nephritis. Intervention of this pathway may become a novel strategy for the treatment of human SLE and possibly other autoimmune diseases.

Acknowledgments

We thank Dr. S. Koyasu (Keio University) for generously supplying DO11.10 TCR transgenic mice.

References

1. Mills, J. A. 1994. Systemic lupus erythematosus. *N. Engl. J. Med. 330:1871.*
2. Kotzin, B. L. 1996. Systemic lupus erythematosus. *Cell 85:303.*
3. Theofilopoulos, A. N., and F. J. Dixon. 1985. Murine models of systemic lupus erythematosus. *Adv. Immunol. 37:269.*
4. Salomon, B., and J. A. Bluestone. 2001. Complexities of CD28/B7: CTLA-4 costimulatory pathways in autoimmunity and transplantation. *Annu. Rev. Immunol. 19:225.*
5. Seo, S. J., M. L. Fields, J. L. Buckler, A. J. Reed, L. Mandik-Nayak, S. A. Nish, R. J. Noelle, L. A. Turka, F. D. Finkelman, A. J. Caton, and J. Erikson. 2002. The impact of T helper and T regulatory cells on the regulation of anti-double-stranded DNA B cells. *Immunity 16:535.*
6. Lenschow, D. J., T. L. Walunas, and J. A. Bluestone. 1996. CD28/B7 system of T cell costimulation. *Annu. Rev. Immunol. 14:233.*
7. Grewal, I. S., and R. A. Flavell. 1996. The role of CD40 ligand in costimulation and T-cell activation. *Immunol. Rev. 153:85.*
8. Van Gool, S. W., P. Vandenberghe, M. de Boer, and J. L. Ceuppens. 1996. CD80, CD86 and CD40 provide accessory signals in a multiple-step T-cell activation model. *Immunol. Rev. 153:47.*
9. Finck, B. K., P. S. Linsley, and D. Wofsy. 1994. Treatment of murine lupus with CTLA4Ig. *Science 265:1225.*
10. Nakajima, A., M. Azuma, S. Kodera, S. Nuriya, A. Terashi, M. Abe, S. Hirose, T. Shirai, H. Yagita, and K. Okumura. 1995. Preferential dependence of autoantibody production in murine lupus on CD86 costimulatory molecule. *Eur. J. Immunol. 25:3060.*
11. Mohan, C., Y. Shi, J. D. Laman, and S. K. Datta. 1995. Interaction between CD40 and its ligand gp39 in the development of murine lupus nephritis. *J. Immunol. 154:1470.*
12. Daikh, D. I., B. K. Finck, P. S. Linsley, D. Hollenbaugh, and D. Wofsy. 1997. Long-term inhibition of murine lupus by brief simultaneous blockade of the B7/CD28 and CD40/gp39 costimulation pathways. *J. Immunol. 159:3104.*
13. Mihara, M., I. Tan, Y. Chuzhin, B. Reddy, L. Budhai, A. Holzer, Y. Gu, and A. Davidson. 2000. CTLA4Ig inhibits T cell-dependent B-cell maturation in murine systemic lupus erythematosus. *J. Clin. Invest. 106:91.*
14. Aten, J., A. Roos, N. Claessen, E. J. Schilder-Tol, I. J. Ten Berge, and J. J. Weening. 2000. Strong and selective glomerular localization of CD134 ligand and TNF receptor-1 in proliferative lupus nephritis. *J. Am. Soc. Nephrol. 11:1426.*
15. Gross, J. A., J. Johnston, S. Mudri, R. Enselman, S. R. Dillon, K. Madden, W. Xu, J. Parrish-Novak, D. Foster, C. Lofton-Day, et al. 2000. TACI and BCMA are receptors for a TNF homologue implicated in B-cell autoimmune disease. *Nature 404:995.*
16. Sporici, R. A., and P. J. Perrin. 2001. Costimulation of memory T-cells by ICOS: a potential therapeutic target for autoimmunity? *Clin. Immunol. 100:263.*
17. Linsley, P. S. 2001. T cell activation: you can't get good help. *Nat. Immunol. 2:139.*
18. Hutloff, A., A. M. Dittrich, K. C. Beier, B. Eljaschewitsch, R. Kraft, I. Anagnostopoulos, and R. A. Kroczek. 1999. ICOS is an inducible T-cell costimulator structurally and functionally related to CD28. *Nature 397:263.*
19. Swallow, M. M., J. J. Wallin, and W. C. Sha. 1999. B7h, a novel costimulatory homolog of B7.1 and B7.2, is induced by TNFα. *Immunity 11:423.*
20. Yoshinaga, S. K., M. Zhang, J. Pistillo, T. Horan, S. D. Khare, K. Miner, M. Sonnenberg, T. Boone, D. Brankow, T. Dai, et al. 2000. Characterization of a new human B7-related protein: B7RP-1 is the ligand to the co-stimulatory protein ICOS. *Int. Immunol. 12:1439.*
21. Ling, V., P. W. Wu, H. F. Finnerty, K. M. Bean, V. Spaulding, L. A. Fouser, J. P. Leonard, S. E. Hunter, R. Zollner, J. L. Thomas, et al. 2000. Cutting edge: identification of GL50, a novel B7-like protein that functionally binds to ICOS receptor. *J. Immunol. 164:1653.*
22. Brodie, D., A. V. Collins, A. Iaboni, J. A. Fennelly, L. M. Sparks, X. N. Xu, P. A. van der Merwe, and S. J. Davis. 2000. LICOS, a primordial costimulatory ligand? *Curr. Biol. 10:333.*
23. Aicher, A., M. Hayden-Ledbetter, W. A. Brady, A. Pezzutto, G. Richter, D. Magaletti, S. Buckwalter, J. A. Ledbetter, and E. A. Clark. 2000. Characterization of human inducible costimulator ligand expression and function. *J. Immunol. 164:4689.*
24. Khayyamian, S., A. Hutloff, K. Buchner, M. Grafe, V. Henn, R. A. Kroczek, and H. W. Mages. 2002. ICOS-ligand, expressed on human endothelial cells, costimulates Th1 and Th2 cytokine secretion by memory CD4$^+$ T cells. *Proc. Natl. Acad. Sci. USA 99:6198.*
25. Yoshinaga, S. K., J. S. Whoriskey, S. D. Khare, U. Sarmiento, J. Guo, T. Horan, G. Shih, M. Zhang, M. A. Coccia, T. Kohno, et al. 1999. T-cell co-stimulation through B7RP-1 and ICOS. *Nature 402:827.*
26. Beier, K. C., A. Hutloff, A. M. Dittrich, C. Heuck, A. Rauch, K. Buchner, B. Ludewig, H. D. Ochs, H. W. Mages, and R. A. Kroczek. 2000. Induction, binding specificity and function of human ICOS. *Eur. J. Immunol. 30:3707.*
27. Dong, C., A. E. Juedes, U. A. Temann, S. Shresta, J. P. Allison, N. H. Ruddle, and R. A. Flavell. 2001. ICOS co-stimulatory receptor is essential for T-cell activation and function. *Nature 409:97.*
28. McAdam, A. J., R. J. Greenwald, M. A. Levin, T. Chernova, N. Malenkovich, V. Ling, G. J. Freeman, and A. H. Sharpe. 2001. ICOS is critical for CD40-mediated antibody class switching. *Nature 409:102.*
29. Tafuri, A., A. Shahinian, F. Bladt, S. K. Yoshinaga, M. Jordana, A. Wakeham, L. M. Boucher, D. Bouchard, V. S. Chan, G. Duncan, et al. 2001. ICOS is essential for effective T-helper-cell responses. *Nature 409:105.*
30. Iwai, H., Y. Kozono, S. Hirose, H. Akiba, H. Yagita, K. Okumura, H. Kohsaka, N. Miyasaka, and M. Azuma. 2002. Amelioration of collagen-induced arthritis by blockade of inducible costimulator-B7 homologous protein costimulation. *J. Immunol. 169:4332.*
31. Sakamoto, S., K. Tezuka, T. Tsuji, N. Hori, and T. Tamatani. 2001. AILIM/ICOS: its expression and functional analysis with monoclonal antibodies. *Hybrid. Hybridomics 20:293.*
32. Knight, J. G., D. D. Adams, and H. D. Purves. 1977. The genetic contribution of the NZB mouse to the renal disease of the NZB × NZW hybrid. *Clin. Exp. Immunol. 28:352.*
33. Kinoshita, K., G. Tesch, A. Schwarting, R. Maron, A. H. Sharpe, and V. R. Kelley. 2000. Costimulation by B7-1 and B7-2 is required for autoimmune disease in MRL-Fas^{lpr} mice. *J. Immunol. 164:6046.*
34. Basgen, J. M., T. E. Nevins, and A. F. Michael. 1989. Quantitation of antigen in tissue by immunofluorescence image analysis. *J. Immunol. Methods 124:77.*
35. Nozawa, K., J. Ohata, J. Sakurai, H. Hashimoto, H. Miyajima, H. Yagita, K. Okumura, and M. Azuma. 2001. Preferential blockade of CD8$^+$ T cell responses by administration of anti-CD137 ligand monoclonal antibody results in differential effect on development of murine acute and chronic graft-versus-host diseases. *J. Immunol. 167:4981.*
36. Sakurai, J., J. Ohata, K. Saito, H. Miyajima, T. Hirano, T. Kohsaka, S. Enomoto, K. Okumura, and M. Azuma. 2000. Blockade of CTLA-4 signals inhibits Th2-mediated murine chronic graft-versus-host disease by an enhanced expansion of regulatory CD8$^+$ T cells. *J. Immunol. 164:664.*
37. Kearney, E. R., K. A. Pape, D. Y. Loh, and M. K. Jenkins. 1994. Visualization of peptide-specific T cell immunity and peripheral tolerance induction in vivo. *Immunity 1:327.*
38. Schuhbauer, D., B. Muller, and A. Mitchison. 1996. Unrepresentative behavior of T cell receptor-transgenic CD4$^+$ T cells upon adoptive transfer: lack of need for priming and an extended booster dose-response. *Immunobiology 195:152.*
39. Hirose, S., N. Maruyama, K. Ohta, and T. Shirai. 1980. Polyclonal B cell activation and autoimmunity in New Zealand mice. I. Natural thymocytotoxic autoantibody (NTA). *J. Immunol. 125:610.*
40. Shirai, T., K. Hayakawa, K. Okumura, and T. Tada. 1978. Differential cytotoxic effect of natural thymocytotoxic autoantibody of NZB mice on functional subsets of T cells. *J. Immunol. 120:1924.*
41. Higuchi, T., Y. Aiba, T. Nomura, J. Matsuda, K. Mochida, M. Suzuki, H. Kikutani, T. Honjo, K. Nishioka, and T. Tsubata. 2002. Cutting edge: ectopic expression of CD40 ligand on B cells induces lupus-like autoimmune disease. *J. Immunol. 168:9.*
42. Liang, L., E. M. Porter, and W. C. Sha. 2002. Constitutive expression of the B7h ligand for inducible costimulator on naive B cells is extinguished after activation by distinct B cell receptor and interleukin 4 receptor-mediated pathways and can be rescued by CD40 signaling. *J. Exp. Med. 196:97.*
43. Ogawa, S., G. Naganatsu, M. Watanabe, S. Watanabe, T. Hayashi, S. Horita, K. Nitta, H. Nihei, K. Tezuka, and R. Abe. 2001. Opposing effects of anti-activation-inducible lymphocyte-immunomodulatory molecule/inducible costimulator antibody on the development of acute versus chronic graft-versus-host disease. *J. Immunol. 167:5741.*
44. Totsuka, T., T. Kanai, R. Iiyama, K. Uraushihara, M. Yamazaki, R. Okamoto, T. Hibi, K. Tezuka, M. Azuma, H. Akiba, et al. 2003. Ameliorating effect of anti-inducible costimulator monoclonal antibody in a murine model of chronic colitis. *Gastroenterology 124:410.*
45. Coyle, A. J., S. Lehar, C. Lloyd, J. Tian, T. Delaney, S. Manning, T. Nguyen, T. Burwell, H. Schneider, J. A. Gonzalo, et al. 2000. The CD28-related molecule ICOS is required for effective T cell- dependent immune responses. *Immunity 13:95.*
46. McAdam, A. J., T. T. Chang, A. E. Lumelsky, E. A. Greenfield, V. A. Boussiotis, J. S. Duke-Cohan, T. Chernova, N. Malenkovich, C. Jabs, V. K. Kuchroo, et al. 2000. Mouse inducible costimulatory molecule (ICOS) expression is enhanced by CD28 costimulation and regulates differentiation of CD4$^+$ T cells. *J. Immunol. 165:5035.*
47. Gonzalo, J. A., J. Tian, T. Delaney, J. Corcoran, J. B. Rottman, J. Lora, A. Al-garawi, R. Kroczek, J. C. Gutierrez-Ramos, and A. J. Coyle. 2001. ICOS is critical for T helper cell-mediated lung mucosal inflammatory responses. *Nat. Immunol 2:597.*
48. Rottman, J. B., T. Smith, J. R. Tonra, K. Ganley, T. Bloom, R. Silva, B. Pierce, J. C. Gutierrez-Ramos, E. Ozkaynak, and A. J. Coyle. 2001. The costimulatory molecule ICOS plays an important role in the immunopathogenesis of EAE. *Nat. Immunol. 2:605.*

Gene Transfer of a Cell Cycle Modulator Exerts Anti-Inflammatory Effects in the Treatment of Arthritis[1]

Yoshinori Nonomura, Hitoshi Kohsaka,[2] Kenji Nagasaka, and Nobuyuki Miyasaka

Forced expression of a cyclin-dependent kinase inhibitor gene, $p21^{Cip1}$ in the synovial tissues was effective in treating animal models of rheumatoid arthritis. Synovial hyperplasia in the treated joints was suppressed, reflecting the inhibitory effect of $p21^{Cip1}$ on cell cycle progression. Additionally, lymphocyte infiltration, expression of inflammatory cytokines, and destruction of the bone and cartilage were inhibited. To determine why the cell cycle regulator gene exerted such anti-inflammatory effects, we investigated gene expression by rheumatoid synovial fibroblasts with or without the $p21^{Cip1}$ gene transferred. We have found that $p21^{Cip1}$ gene transfer down-regulates expression of various inflammatory mediators and tissue-degrading proteinases that are critically involved in the pathology of rheumatoid arthritis. These molecules included IL-6, -8, type I IL-1R (IL-1R1), monocyte chemoattractant protein-1, macrophage inflammatory protein-3α, cathepsins B and K, and matrix metalloproteinases-1 and -3. Down-regulation of IL-1R1 by $p21^{Cip1}$ resulted in attenuated responsiveness to IL-1. Inhibition of the inflammatory gene expression by $p21^{Cip1}$ was seen even when IL-1 is absent. This IL-1R1-independent suppression was accompanied by reduced activity of c-Jun N-terminal kinase, which was associated with $p21^{Cip1}$, and inactivation of NF-κB and AP-1. These multiple regulatory effects should work in concert with the primary effect of inhibiting cell cycle in ameliorating the arthritis, and suggest a heretofore unexplored relationship between cyclin-dependent kinase inhibitor gene and inflammatory molecules. ***The Journal of Immunology,*** **2003, 171: 4913–4919.**

Synovial tissue from healthy individuals consists of a single layer of synovial cells without infiltration of inflammatory cells. In rheumatoid synovial tissue, lymphocytes and macrophages are recruited and activated, and these activated macrophages release high concentrations of inflammatory cytokines. In response to these cytokines, synovial fibroblasts proliferate vigorously and form villous hyperplastic synovial tissues. These fibroblasts secrete inflammatory mediators, which further attract inflammatory cells and stimulate growth of the synovial fibroblasts as well as that of vascular endothelial cells (1). These activated macrophages and fibroblasts produce tissue-degrading proteinases (2). Thus, the invasive hyperplastic synovial tissue, termed pannus, is directly responsible for structural and functional damage of the affected joints.

Therapeutic intervention against rheumatoid arthritis (RA)[3] could be aimed at any one of these steps. Recently developed biological reagents that block activities of TNF-α have proved to be beneficial in clinical settings. However, they and other conventional drugs do not necessarily control synovial inflammation and hyperplasia in all patients. We hypothesized that the proliferation of the synovial fibroblasts is a common outcome of the multiple inflammatory processes in RA. If synovial fibroblasts become refractory to the proliferative stimuli, the tissue-degrading pannus should not develop. This idea led us to explore new therapeutic approaches that directly control synovial cell proliferation (3–5). The molecules we have focused on are cyclin-dependent kinase inhibitors (CDKIs). These intracellular proteins inhibit kinase activity of cyclin/cyclin-dependent kinase (CDK) complexes that are required for cell cycle progression (6).

Our previous studies have shown that CDKIs $p16^{INK4a}$ and $p21^{Cip1}$ are not expressed in vivo in the rheumatoid synovial tissues, but readily induced in vitro in cultured rheumatoid synovial fibroblasts (RSF). Induction of $p16^{INK4a}$ is characteristic of RSF (3). In vitro inducibility of $p16^{INK4a}$ and $p21^{Cip1}$ suggested to us that their induction in vivo in the rheumatoid joints could be an ideal approach to suppression of the proliferative synovitis. This was substantiated by intraarticular transfer of the $p16^{INK4a}$ or $p21^{Cip1}$ gene to rodent models of RA (4, 5). These gene therapies suppressed synovial hyperplasia and also inhibited lymphocyte infiltration and destruction of the bone and cartilage of the treated joints. Expression of inflammatory cytokines such as IL-1, -6 and TNF-α was suppressed even in the small amount of hyperplastic synovial tissues that remained after the gene transfer (4). These data argued that induction of CDKI ameliorated the arthritis not only by inhibition of cell cycle but by other unknown functions that suppressed the inflammatory network in the arthritic joint.

Unlike the other CDKIs, $p21^{Cip1}$ binds to various molecules related to gene expression and exerts differential effects on different cells (7). However, little is known about the effects of $p21^{Cip1}$ on gene expression in the inflamed tissues. We show here that up-regulated expression of the $p21^{Cip1}$ gene in RSF suppresses expression of various inflammatory molecules that play critical roles in the pathology of RA. Manipulation of these multiple

Department of Bioregulatory Medicine and Rheumatology, Graduate School, Tokyo Medical and Dental University, Tokyo, Japan

Received for publication December 30, 2002. Accepted for publication August 20, 2003.

The costs of publication of this article were defrayed in part by the payment of page charges. This article must therefore be hereby marked *advertisement* in accordance with 18 U.S.C. Section 1734 solely to indicate this fact.

[1] This work was supported by grants from the Japanese Ministry of Health, Labor and Welfare, from the Japanese Ministry of Education, Culture, Sports, Science and Technology, Japan, and from the Kato Memorial Bioscience Foundation.

[2] Address correspondence and reprint requests to Dr. Hitoshi Kohsaka, Bioregulatory Medicine and Rheumatology, Graduate School, Tokyo Medical and Dental University, 1-5-45 Yushima, Bunkyo-ku, Tokyo 113-8519, Japan. E-mail address: kohsaka.rheu@tmd.ac.jp

[3] Abbreviations used in this paper: RA, rheumatoid arthritis; CDKI, cyclin-dependent kinase inhibitor; CDK, cyclin/cyclin-dependent kinase; RSF, rheumatoid synovial fibroblast; IL-1ra, IL-1R antagonist; JNK, c-Jun N-terminal kinase; IL-1R1, type I IL-1R; MCP, monocyte chemoattractant protein; MMP, matrix metalloproteinase; MIP, macrophage inflammatory protein; TLR, Toll-like receptor.

0022-1767/03/$02.00

molecular events should contribute to the therapeutic effects of p21^{Cip1} gene therapy.

Materials and Methods

Cell culture and recombinant adenoviruses

Synovial tissues were obtained from patients who had responded poorly to anti-rheumatic drugs and underwent joint replacement or synovectomy for active rheumatoid synovitis at Tokyo Medical and Dental University Hospital (Tokyo, Japan), Tokyo Metropolitan Bokuto, or Fuchu Hospital (Tokyo, Japan). The patients fulfilled the American College of Rheumatology criteria for classification of RA (8). All patients gave their consent for all procedures in the present studies, which were also approved by the ethics committee of Tokyo Medical and Dental University. From villous and congestive synovial tissues, RSF were isolated and cultured as described elsewhere (3). They were used at passages 3–11. RSF were infected with AxCAp21 adenovirus, containing a human p21^{Cip1} gene (5, 9), or Ax1w1 adenovirus (Riken Gene Bank, Saitama, Japan), which lacks insert genes, at 50 multiplicity of infection. Some RSF were stimulated by 5 ng/ml TNF-α (Genzyme, Cambridge, MA), 5 ng/ml IL-1β (PeproTech, Rocky Hill, NJ), and 25 μM indomethacin (Sigma-Aldrich, St. Louis, MO). In preliminary experiments, 5 ng/ml was determined to be the optimal concentration for each cytokine to stimulate RSF. RNeasy kit (Qiagen, Valencia, CA) with DNase I treatment was used to isolate total RNA. For ELISA, the virus-infected RSF were cultured for three days, transferred to microwells at 1.0×10^5 cells/ml, and incubated for 12 h. After replacement of the culture medium, RSF were further cultured for 24 h with 10% serum alone, 5 ng/ml IL-1β together with 25 μM indomethacin, 5 ng/ml TNF-α, a combination of IL-1β, indomethacin, and TNF-α, or 5 μg/ml LPS of *Escherichia coli* O55:B5 (Sigma-Aldrich). One hundred ng/ml IL-1R antagonist (IL-1ra) (R&D Systems, Mckinley, MN), which was sufficient for the inhibition of 10 pg/ml IL-1β, was added to some wells. The culture supernatants were collected after 24 h. For Western blotting, RSF were lyzed for protein extraction at three days after the adenoviral infection (3). To assess transcription factor and c-Jun N-terminal kinase (JNK) activities in RSF that were incubated for 30 min in the medium containing 10% FBS with or without supplementation of 5 μg/ml LPS, nuclear extracts and cell lysates were prepared using Nuclear Extract Kit (Active Motif, Carlsbad, CA) or SAPK/JNK assay kit (Cell Signaling, Beverly, MA). The effects of the p21^{Cip1} gene were studied at three days after the adenoviral infection.

Northern blot analyses

Northern blotting was conducted as described elsewhere (10). Human monocyte chemoattractant protein (MCP)-1 cDNA (No. 65933, American Type Culture Collection, Manassas, VA), human GAPDH cDNA (Life Technologies, Rockville, MD), and PCR products of type I IL-1R (IL-1R1), cathepsins B and K, and matrix metalloproteinases (MMP)-1 and -3 were used as probes. Fragments of IL-1R1, cathepsins B and K, and MMPs-1 and -3 cDNA were generated with RT-PCR using cDNA derived from RSF. PCR was conducted with *Taq* polymerase (Life Technologies) and sets of specific primers: human IL-1R1-specific primers (11), human MMP-1-specific primers (12), human MMP-3-specific primers (12), human cathepsin B-specific primers (5′-TAG GAT CTG GCT TCC AAC AT-3′ (sense) and 5′-CCA CGG CAG ATT AGA TCT TT-3′ (antisense)) and human cathepsin K-specific primers (5′-AAC GAA GCC AGA CAA CAG ATT TCC-3′ (sense), 5′-GAT TTG GCT GGC TGG AGT CAC A-3′ (antisense)). Annealing temperatures were 58°C for IL-1R1, and cathepsins B and K cDNA, and 60°C for MMP-1 and -3 cDNA. The products were purified and labeled with [α-^{32}P]dATP (Amersham Biosciences, Buckinghamshire, UK) and hybridized with the Northern blot membranes. Digital image files were generated with Phosphorimaging Screens and the BAS-2500 PhosphoImager, and analyzed with MacBAS 2.5.2 Software (Fuji Film, Kanagawa, Japan).

Western blot analyses and immunoprecipitation

Rabbit anti-human IL-1R1 Abs, rabbit anti-human Toll-like receptor (TLR)-4 Abs, and rabbit anti-human p21^{Cip1} Abs (sc-688, sc-10741 and sc-387, respectively, Santa Cruz Biotechnology, Santa Cruz, CA) were used as primary Abs for Western blot analyses. HRP-conjugated anti-rabbit IgG polyclonal Abs (NA-934, Amersham Biosciences) were used as the secondary Abs. Bound Abs were visualized with ECL or ECL-plus (Amersham Biosciences). Signal intensities were quantified with NIH Image ver. 1.62 (National Institutes of Health, Bethesda, MD). JNKs 1–3 were immunoprecipitated using mouse anti-human JNK2 Ab (sc-7345, Santa Cruz Biotechnology) (13).

ELISA

ELISA kits for IL-1β, IL-6, IL-8, MCP-1, TNF-α (BioSource International, Camarillo, CA), IL-1α, macrophage inflammatory protein (MIP)-3α (R&D Systems), MMP-1 (Amersham Biosciences) and MMP-3 (Fuji Chemical, Toyama, Japan) were used to quantify the protein levels in the culture supernatants.

Multiwell colorimetric transcription factor assays and JNK kinase assay

Using Trans AM AP-1/c-Jun, NF-κBp50, and p65 Transcription Factor Assay Kits (Active Motif), the nuclear extracts of RSF were examined for DNA binding activities of AP-1 and NF-κB (14). SAPK/JNK Assay Kit (Cell Signaling) was used to examine whole cell lysates for their JNK kinase activities to phosphorylate c-Jun substrates. The amount of the c-Jun substrate was standardized by immunoblotting with anti c-Jun Ab (sc-44, Santa Cruz Biotechnology).

Statistics

Signal intensity ratios of Northern and Western blot analyses, and protein concentrations were compared with a paired Student's *t* test using StatView-5.0J software (SAS Institute, Cary, NC).

Results

p21^{Cip1} suppresses IL-1R1 and IL-6 expression by RSF

RSF samples derived from rheumatoid joints were cultured in vitro. Expression of p21^{Cip1} was not detected in any of the samples. They were infected with the AxCAp21 adenoviruses or the Ax1w1 adenoviruses. At three days postinfection, when the AxCAp21-infected RSF express p21^{Cip1} at the highest level, the cells were harvested for RNA and protein extraction.

In preliminary experiments using a few RSF samples and commercial DNA array systems, MCP-1, IL-1R1, and cathepsins B and K genes, which are related to RA pathology, showed a tendency to be down-regulated by the p21^{Cip1} gene transfer. Indeed, Northern blot analysis revealed that the IL-1R1 mRNA expression was significantly reduced in RSF overexpressing p21^{Cip1}, compared with those infected with the control adenoviruses (Fig. 1*A*). Reflecting this, Western blot analyses of the total cell lysates showed that the IL-1R1 protein expression was reduced in the RSF expressing p21^{Cip1} (Fig. 1*B*).

The DNA array analyses suggested no differential expression of IL-6 in the unstimulated RSF. However, when RSF were stimulated by TNF-α and IL-1β before the DNA array analysis, IL-6, as well as IL-8, MCP-1, MIP-3α, MMP-1, MMP-3, and cathepsin K genes showed a tendency to be down regulated by p21^{Cip1}. This was consistent with the fact that TNF-α and IL-1, both of which are critically involved in activating RSF in the rheumatoid joints, stimulate RSF to promote secretion of various cytokines including IL-6 (15). The unstimulated RSF did not release IL-1α, IL-1β, or TNF-α above the lowest limit of detection in the ELISA (3.9 pg/ml). These facts implied that the suppression of IL-6 in the stimulated RSF could be attributable to the down-regulation of IL-1R1. To address this issue, RSF were stimulated independently with IL-1β, TNF-α, or a combination of the two. The culture supernatants were examined for the IL-6 concentration with ELISA. Each stimulation promoted IL-6 production. The effects of IL-1β were suppressed significantly by p21^{Cip1} while the effects of TNF-α were not attenuated (Fig. 1*C*). Effects of the adenoviral infection alone on the IL-6 secretion were minimal (Fig. 1*D*). Thus, the down-regulation of IL-1R1 was biologically relevant to the suppression of IL-6.

To determine whether other pathways that regulate IL-6 production are affected, RSF were stimulated with LPS. Western blot analysis confirmed that Toll-like receptor (TLR)4, which is a receptor for LPS, was not down-regulated by p21^{Cip1} (Fig. 1*E*). Nevertheless, the p21^{Cip1} expression suppressed the IL-6 production

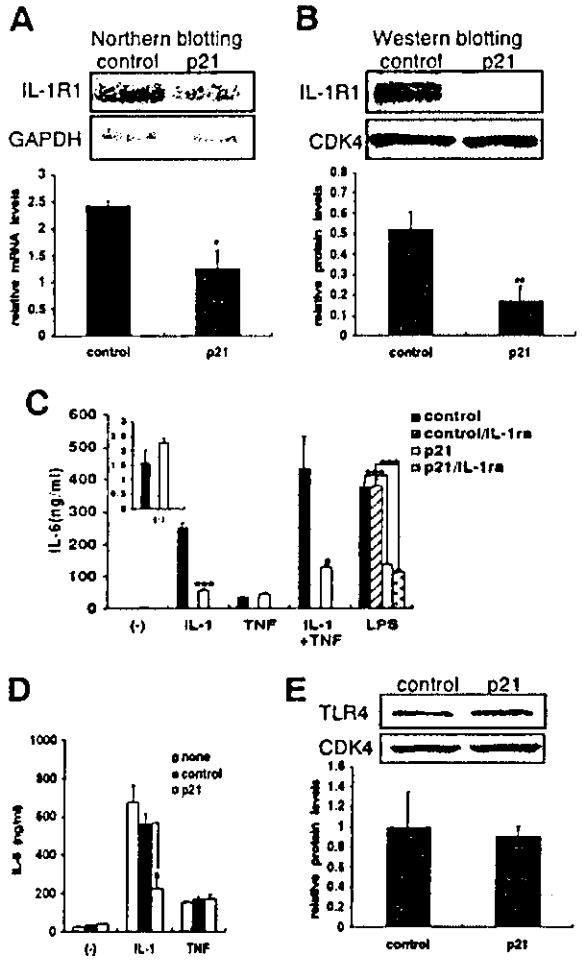

FIGURE 1. Suppression of inflammatory cytokine and cytokine receptor expression by p21^{Cip1}. *A*, RNA from the p21^{Cip1} adenovirus-infected (p21) and control adenovirus-infected RSF (control) were examined for IL-1R1 and GAPDH mRNA expression by Northern blot analysis. Representative blots of one of three samples are shown in the upper panel. Signal intensities of IL-1R1 were normalized with those of GAPDH (relative mRNA levels), and are shown in the lower panel. The columns and bars represent the mean and SD of three samples. Mean reduction by p21^{Cip1} was 48.2%. Statistical evaluation was conducted by paired Student's *t* test. *, $p < 0.05$. *B*, The cells from the same donor were examined for IL-1R1 and CDK4 protein expression by Western blot analysis. Representative blots of one of three samples are shown in the *upper panel*. Signal intensities of IL-1R1 protein were normalized with those of constitutively expressed CDK4 (relative protein levels), and are shown in the *lower panel*. Mean reduction of expression by p21^{Cip1} was 67.6%. **, $p < 0.01$. *C*, RSF infected with the p21^{Cip1} adenoviruses (open columns), and infected with the control adenoviruses (solid columns) were cultured without stimulation (−) or stimulated with IL-1β (IL-1), TNF-α (TNF), or combination of IL-1β and TNF-α (IL-1+TNF) for 24 h. RSF were stimulated with LPS for 24 h in a separate set of experiments, where some RSF were treated with IL-1ra after the infection with the control adenoviruses (hatched column) or with the p21 adenoviruses (dotted column). IL-6 in the culture supernatants was measured by ELISA. Representative data of three independent experiments are shown. Columns and bars show the mean and SD of triplicate cultures. Mean reduction of expression by p21^{Cip1} in IL-1, IL-1+TNF, LPS, and LPS+IL-1ra were 77.4, 64.3, 69.4, and 64.3%, respectively. *, $p < 0.05$ and ***, $p < 0.005$. *D*, RSF infected with the p21^{Cip1} adenoviruses (open columns), and infected with the control adenoviruses (solid columns) and noninfected RSF (gray column) were cultured without stimulation (−) or stimulated with IL-1β (IL-1) or TNF-α (TNF) for 24 h. IL-6 in the culture supernatants was measured by ELISA. Representative data of two experiments are shown. Columns and bars show the mean and SD of triplicate cultures. No statistical differences were found between IL-6 production by control-virus infected RSF and that by noninfected RSF. *E*, Expression of TLR4 and CDK4 proteins was analyzed by Western blot analysis. Representative blots of one of three samples are shown. The relative protein levels of TLR4 to CDK4 are shown as columns and bars. TLR4 protein level was not suppressed by p21^{Cip1}.

that was induced by LPS (Fig. 1*C*). Again, the culture supernatants of the LPS-stimulated RSF did not contain detectable amounts of IL-1 (<3.9 pg/ml) or TNF-α (<1.7 pg/ml). To eliminate the effect of a trace amount of IL-1 that might possibly have been secreted with the LPS stimulation, 100 ng/ml IL-1ra, a competitive inhibitor of IL-1α and IL-1β, was added to the culture. This treatment did not alter the results whereas the same concentration of IL-1ra suppressed the IL-6 production by RSF that were stimulated with 10 pg/ml IL-1β (data not shown).

p21^{Cip1} suppresses inflammatory chemokine expression by RSF

The p21^{Cip1}-induced reduction of the MCP-1 mRNA expression by unstimulated RSF was elucidated by Northern blot analyses (Fig. 2*A*). This was reflected in the reduced MCP-1 concentration in the culture supernatants of the p21^{Cip1}-expressing RSF. As was the case in the IL-6 expression, addition of IL-1ra did not alter the results (Fig. 2*B*).

ELISA of MCP-1 in the culture supernatants of RSF stimulated with IL-1β and TNF-α validated the stimulatory effects of these cytokines, and also suppression by p21^{Cip1} (Fig. 2*C*). The effect of IL-1β was significantly suppressed by the p21^{Cip1}expression, while that of TNF-α was unchanged (Fig. 2*C*). These results confirmed the biological significance of the IL-1R1 down-regulation. Furthermore, LPS stimulated RSF to increase MCP-1 production. This was suppressed by p21^{Cip1}. Addition of IL-1ra did not attenuate the LPS-induced production of MCP-1. Thus, the suppression in this setting was also independent of IL-1 (Fig. 2*C*).

In accordance with the results of the preliminary DNA array analysis, MIP-3α or IL-8 protein levels were suppressed by p21^{Cip1} in the culture supernatants of RSF only when they were stimulated with IL-1β and TNF-α. The effect of IL-1β was significantly reduced by the p21^{Cip1} expression, while that of TNF-α was unchanged. LPS also stimulated MIP-3α production. This IL-1-independent effect was partially inhibited by p21^{Cip1}. Similarly, the production of IL-8 was increased both by IL-1β and TNF-α. The effect of IL-1β but not that of TNF-α was inhibited by p21^{Cip1}. LPS exerted a stimulatory effect on IL-8 production comparable to that of TNF-α, which was inhibited significantly by p21^{Cip1}.

p21^{Cip1} suppresses expression of tissue-degrading proteinases

Northern blot analyses confirmed that p21^{Cip1} suppresses expression of cathepsins B and K in the unstimulated RSF, and that of MMP-1 and -3 in the stimulated RSF (Fig. 3, *A–D*).

These changes were reproduced when the concentrations of MMP-1 and -3 in the culture supernatants were determined (Fig. 3, *E* and *F*). Neither MMP was detected in the supernatants of the unstimulated RSF. MMP-1 production was increased by IL-1β and TNF-α. The combination of these two cytokines had a synergistic effect. The effects of IL-1 were significantly suppressed by p21^{Cip1}. As was the case in the cytokine production, LPS increased production of MMP-1. This effect was partially suppressed by p21^{Cip1}. The production MMP-3 was increased by IL-1β and LPS. TNF-α alone had no apparent effect but showed a synergistic effect with IL-1β. Again, the effect of IL-1β was suppressed by p21^{Cip1}, and the effect of LPS was abrogated completely by p21^{Cip1}.

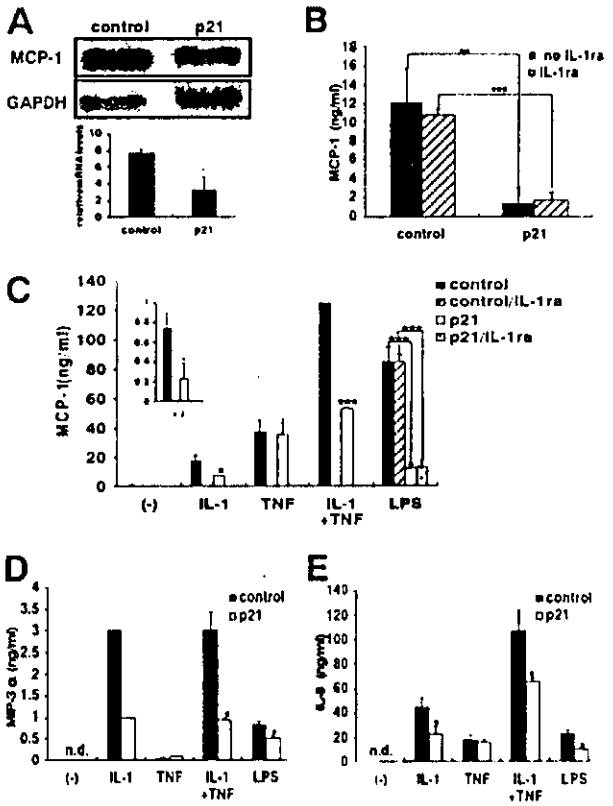

FIGURE 2. Suppression of inflammatory chemokine expression by p21^{Cip1}. *A*, The AxCAp21 adenovirus-infected (p21) and control adenovirus-infected (control) RSF from three RA patients were examined for MCP-1 mRNA expression by Northern blot analysis. RSF were not stimulated with cytokines. Representative results of one of three samples are shown in the *upper panel*. Signal intensities of MCP-1 messages normalized with those of GAPDH messages (relative mRNA levels) are shown as columns and bars, representing the mean and SD. Mean reduction of expression by p21^{Cip1} was 57.0%. *, $p < 0.05$. *B*, RSF with or without p21^{Cip1} expression (p21 and control) were cultured without cytokine stimulation. The culture medium was supplemented with FBS alone (solid columns) or with FBS plus IL-1ra (hatched columns). MCP-1 in the culture supernatants was measured by ELISA. Representative data of two experiments are shown. Columns and bars show the mean and SD of triplicate cultures. Mean reduction of expression by p21^{Cip1} was 83.8% (no IL-1ra) and 87.1% (IL-1ra). **, $p < 0.01$ and ***, $p < 0.005$. *C-E*, RSF infected with the p21^{Cip1} adenoviruses (open columns) or control adenoviruses (solid columns) were cultured without stimulation (−) or stimulated with IL-1β (IL-1), TNF-α (TNF), a combination of IL-1β and TNF-α (IL-1+TNF), or LPS for 24 h. Some RSF infected with the control adenoviruses (hatched column), and with the p21 adenoviruses (dotted column) were treated with IL-1ra before LPS stimulation. MCP-1 (C), MIP-3α (D), and IL-8 (E) in the culture supernatants were measured by ELISA. Representative data of two or three experiments are shown. Columns and bars show the mean and SD of triplicate cultures. n. d., not detectable. Mean reduction in expression of MCP-1 by p21^{Cip1} in IL-1, IL-1+TNF, LPS, and LPS + IL-1ra was 58.3, 57.5%, 84.7, and 83.9%, respectively. Mean reduction in expression of IL-8 by p21^{Cip1} in IL-1, IL-1+TNF, and LPS was 48.4, 38.2, and 54.0% and that of MIP-3α was 66.6, 68.7, and 38.7%. *, $p < 0.05$ and ***, $p < 0.005$.

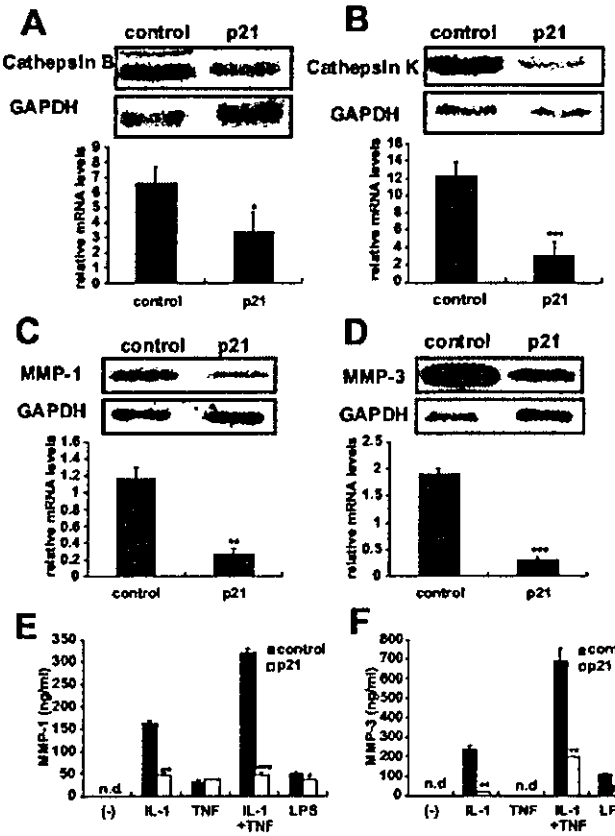

FIGURE 3. Suppression of tissue-degrading proteinase expression by p21^{Cip1}. *A* and *B*, RSF infected with the AxCAp21 adenoviruses (p21) or control adenoviruses (control) were cultured without cytokine stimulation, and examined for cathepsins B (*A*) and K (*B*) mRNA expression by Northern blot analysis. Representative blots are shown in the *upper panels*. Northern blots of cathepsin B showed dual bands representing two transcripts 4.0 and 2.2 kb long (48). The relative levels of mRNA to those of GAPDH mRNA are shown as columns and bars, representing the mean and SD of three samples derived from different patients. Mean reduction in expression of cathepsins B and K by p21^{Cip1} was 47.8 and 75.0%, respectively. *, $p < 0.05$ and ***, $p < 0.005$. *C* and *D*, RSF stimulated with IL-1β and TNF-α were examined for MMP-1 (*C*) and -3 (*D*) mRNA expression by Northern blot analysis. Representative blots of one of three samples are shown in the *upper panels*. The relative levels of mRNA of MMP-1 and -3 are shown as columns and bars, representing the mean and SD of three samples. Mean reduction in expression of MMP-1 and -3 by p21^{Cip1} was 78.6 and 82.6%, respectively. **, $p < 0.01$ and ***, $p < 0.005$. *E* and *F*, RSF infected with the p21^{Cip1} adenoviruses (open columns), and with the control adenoviruses (solid columns) were cultured without stimulation (−) or stimulated with IL-1β (IL-1), TNF-α (TNF), a combination of IL-1β and TNF-α (IL-1+TNF), or LPS for 24 h. MMP-1 and -3 in the culture supernatants were measured by ELISA. Representative data of two experiments are shown. Columns and bars show the mean and SD of triplicate cultures. Unstimulated RSF produced no detectable MMP-1 or -3. Mean reduction in expression of MMP-1 by p21^{Cip1} in IL-1, IL-1+TNF, and LPS was 70.9, 85.3, and 29.5%, respectively, and that of MMP-3 was 92.6, 71.5, and 88.3%, respectively. *, $p < 0.05$; **, $p < 0.01$; ***, $p < 0.005$.

p21^{Cip1} inhibits DNA binding activity of AP-1 and NF-κB

p21^{Cip1} down-regulated expression of MCP-1 and cathepsins B and K in the unstimulated RSF. Although it did not suppress expression of TLR4, it suppressed the LPS-dependent up-regulation of many inflammatory mediators. This has led us to assume that p21^{Cip1} should directly inhibit nonreceptor, intracellular molecules. Since promoter activity of the inflammatory mediator genes that were suppressed by p21^{Cip1} is controlled mostly by NF-κB and AP-1 transcription factors, we investigated the DNA binding activities of these factors in the unstimulated and LPS-stimulated RSF. Multiwell colorimetric assays to quantify DNA binding activity of the transcription factors showed that activity of AP-1 was down-regulated by p21^{Cip1} in the unstimulated RSF. Stimulation

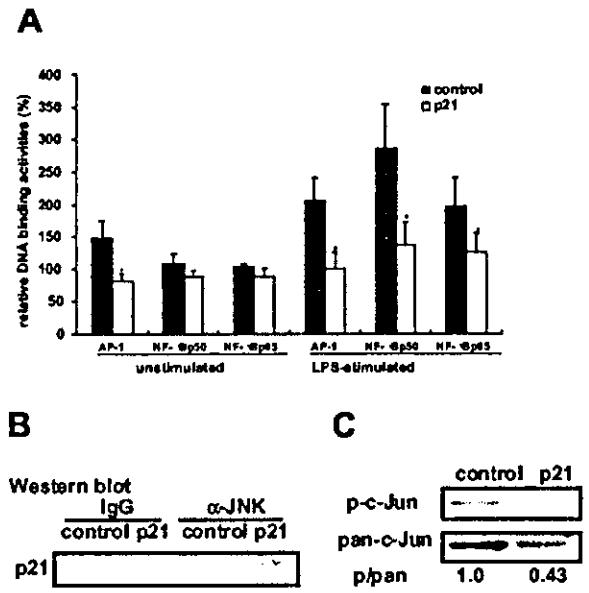

FIGURE 4. Suppression of AP-1 and NF-κB transcription factors by $p21^{Cip1}$. RSF infected with the $p21^{Cip1}$ adenoviruses (p21) or control adenoviruses (control) were cultured with or without LPS stimulation. The DNA binding activities of AP-1 and NF-κB in the adenoviruses-infected RSF relative to those of the uninfected RSF without stimulation are shown (A). Columns and bars show the mean and SD of triplicate cultures. $p21^{Cip1}$ suppressed DNA binding activity of AP-1, but did not suppress that of NF-κBp50 or p65 significantly in the unstimulated RSF. Mean reduction in expression of the AP-1 activity was 47.3%. In the LPS-stimulated RSF, $p21^{Cip1}$ suppressed DNA binding activities of AP-1, NF-κBp50, and p65. Mean reduction in expression of AP-1, NF-κBp50, and NF-κB p65 by $p21^{Cip1}$ was 47.4, 52.6, and 41.3%, respectively. *, $p < 0.05$. $p21^{Cip1}$ in the $p21^{Cip1}$-expressing RSF stimulated with LPS (p21) was coimmunoprecipitated with anti-JNK Ab (α-JNK), but not with control IgG (IgG). No precipitation was found when RSF were infected with the control viruses (control) (*B*). Phosphorylation of c-Jun (p-c-Jun) was suppressed in RSF infected with the $p21^{Cip1}$ viruses (p21) but not in RSF infected with the control viruses (control). Reduction in expression of relative p-c-Jun levels to whole c-Jun (pan-c-Jun) was 57% (*C*). The results are representatives of two independent experiments.

with LPS up-regulated activities of NF-κB p50, p65, and AP-1, all of which were down-regulated by $p21^{Cip1}$ (Fig. 4*A*).

It was shown that $p21^{Cip1}$ associates with JNK in other type of cells, which results in reduction of the JNK enzymatic activity that activates AP-1 (16). Using anti-JNK Ab, we immunoprecipitated JNK in cell lysates of $p21^{Cip1}$-expressing RSF that were stimulated with LPS. Immunoblotting of the precipitants with anti-$p21^{Cip1}$Abs revealed that $p21^{Cip1}$ indeed associated with JNK (Fig. 4*B*). Phosphorylation of c-Jun substrates showed that kinase activity of JNK was suppressed in the $p21^{Cip1}$-expressing RSF (Fig. 4*C*). Thus, the IL-1R1-independent suppression should be at least partly due to down-regulation of these pathways.

Discussion

Since the primary function of CDKIs is the inhibition of kinase activity of CDKs, the anticipated effect of the $p21^{Cip1}$ expression in RSF was suppression of cell cycle progression. Indeed, RSF infected with the AxCAp21 viruses did not respond in vitro to proliferative stimuli by proinflammatory cytokines or by growth factors (4). In vivo transfer of the $p21^{Cip1}$ gene into the arthritic joints of RA model rats suppressed synovial hyperplasia and cell cycle progression of the synovial fibroblasts (5).

However, the present study has revealed that $p21^{Cip1}$ exerts multiple auxiliary effects: down-regulation of cytokine, chemokine, cytokine receptor, and proteinase expression critically involved in the pathology of RA. We found previously that expression of proinflammatory cytokines such as IL-1, IL-6, and TNF-α was unexpectedly inhibited in vivo in the synovial tissues treated with $p21^{Cip1}$ gene transfer (4). The present report provides molecular evidence showing that $p21^{Cip1}$ expression has a wide array of anti-inflammatory and bone-protective effects. Down-regulation of IL-1R1, and also IL-1R-independent inactivation of intracellular signaling pathways appeared to account for these effects (Fig. 5). Finally, these effects suggest that the $p21^{Cip1}$ gene transfer might ameliorate types of inflammatory arthritides other than RA.

The down-regulation of IL-6 observed in vivo was actually seen in vitro in $p21^{Cip1}$-expressing RSF while the expression of IL-1 or TNF-α were not significantly modulated. It is possible that the decreased expression of IL-1 and TNF-α in the synovial tissues was due to their down-regulation in the synovial macrophages. The macrophages are the primary source of these cytokines and, together with synovial fibroblasts, were targeted by the intraarticular adenoviral gene transfer (15, 17). Alternatively, the down-regulation of IL-1 and TNF-α might result from en bloc suppression of the inflammatory cytokine/chemokine network, multiple members of which were suppressed by $p21^{Cip1}$.

IL-6, in the rheumatoid synovial tissues, derives from the activated synovial macrophages and fibroblasts, and stimulates local osteoclasts to resorb the bone matrices in the affected joints. It also stimulates T and B lymphocytes. This has made this cytokine the target of a new biological reagent that is currently in clinical trials (18, 19). IL-8 produced by the activated synovial cells contributes to recruitment of neutrophils and T lymphocytes and to neovascularization in the rheumatoid tissues (20). The other chemokines, MCP-1 and MIP-3α, both evoke migration and activation of lymphocytes and macrophages in the rheumatoid synovial tissues (21, 22). Blockage of MCP-1 receptor was effective in treating an animal model of RA (23). Thus, the cytokines and chemokines down-regulated by $p21^{Cip1}$ all play crucial roles in the rheumatoid inflammation.

Tissue degrading enzymes, such as MMPs and cathepsins, are abundantly expressed in rheumatoid synovial tissues. MMP-1 and -3 degrade collagen and proteoglycans that compose the matrices of bone and cartilage. In addition, it has been proposed that MMP-3 cleaves many proMMPs in the initiation of the proteinase cascade in rheumatoid joints (2). Treatment to inhibit MMP-1 production prevented bone destruction in adjuvant arthritis of rats

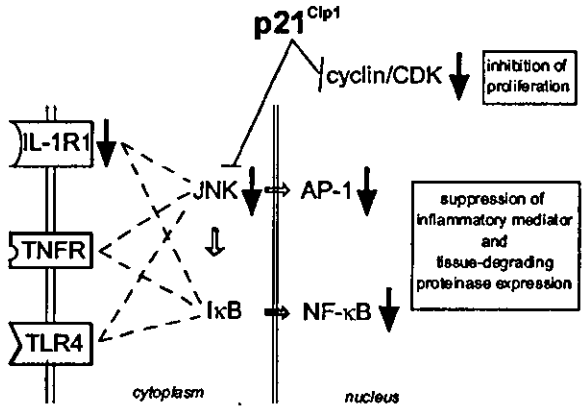

FIGURE 5. Multiple effects of $p21^{Cip1}$ on RSF. $p21^{Cip1}$ inhibited kinase activity of cyclin/CDK complexes, and down-regulated IL-1R1 expression and DNA binding activities of NF-κB and AP-1. These effects were mediated at least by binding of $p21^{Cip1}$ to cyclin/CDK complexes and JNK, and resulted in inhibition of proliferation and in suppression of IL-6, -8, MCP-1, MIP-3α, cathepsins B and K, and MMP-1 and -3 expression.

(24). Cathepsin B might contribute to rheumatoid joint damage by degrading collagen (25, 26, 27). Cathepsin K is not only expressed by osteoclasts, but also by synovial fibroblasts, contributing to bone destruction in the rheumatoid joints (28, 29). Down-regulation of these proteinases in the p21^{Cip1}-expressing RSF was consistent with the remarkable inhibition of bone and cartilage degeneration observed in the p21^{Cip1} gene therapy.

Expression of IL-1R1 was suppressed by p21^{Cip1}. IL-1 is one of the critical cytokines in the rheumatoid inflammation. It enhances migration of inflammatory cells into the synovial tissues and stimulates production of cytokines, chemokines and MMPs (15). Its blockade by an antagonist ameliorates RA (30–32). We saw that IL-1-triggered promotion of IL-6, IL-8, MCP-1, MIP-3α, and MMP-1 and -3 release from RSF was significantly suppressed by p21^{Cip1}. These results argue that down-regulation of IL-1R1 must be functionally relevant to the therapeutic effects.

MCP-1 and cathepsin B and K expression was suppressed even when RSF were not stimulated. Conventional ELISA detected no IL-1 in the culture supernatant of the unstimulated RSF. The blockade of IL-1 with IL-1ra did not affect the results. Thus, the suppression observed in the unstimulated RSF was not mediated by the down-regulation of IL-1R1. LPS also up-regulated MCP-1 expression, and induced expression of IL-6, IL-8, MIP-3α, and MMP-1 and -3. This was not accompanied by reduced expression of TLR4, which is a signaling receptor for LPS. The LPS-stimulated RSF under these conditions did not release a detectable level of IL-1 into the culture supernatants, and IL-1 blockade by IL-1ra did not alter the results. Thus, inhibition of the inflammatory molecule expression could be at least partly due to modulation of intracellular pathways that are independent of IL-1R1. IL-1 and TNF-α have distinct pathways in the afferent arm of the signal transduction whereas IL-1 and LPS share a part of the signal transduction molecules (33). Presumably, this difference should account for the distinct effect of p21^{Cip1} on TNF-α and LPS stimulation.

The IL-1R-independent suppression was accompanied by reduced activity of NF-κB and AP-1. In the rheumatoid synovial tissues these factors activate transcription of various inflammatory cytokines, chemokines, and proteinases including those analyzed in the present studies (17, 24, 34–42). In agreement with our observation, constitutive expression of MCP-1 by mesangial cells required activation of AP-1 (43). Notably, the promoter of the *IL-1R1* gene has two AP-1-like binding sites (44). This suggests that the repressed activity of AP-1 might contribute to the down-regulation of IL-1R1.

Depending on the cell type, p21^{Cip1} binds to a variety of intracellular proteins other than CDKs. These include signal transduction molecules and transcription factors (7). We have shown that p21^{Cip1} indeed binds to JNK and suppresses its kinase activity in RSF. It is known that JNK could activate NF-κB by degrading Iκ-B (45, 46). Thus, interaction of p21^{Cip1} with mitogen-activated protein kinase might account for the reduced activity of AP-1 and NF-κB.

Chang et al. (47) used the DNA array technique to study effects of p21^{Cip1} on gene expression in HT1080 human sarcoma cell line; they observed that genes related to senescence or age-related diseases were induced. We have shown here that p21^{Cip1} expression modulates the expression of genes related to inflammation. Although, Chang et al. found up-regulation of the *cathepsin B* gene in HT1080 cells, the same gene was down-regulated in RSF. It is probable that the effects of p21^{Cip1} depend on the cell types.

In conclusions, p21^{Cip1} gene transfer to the RSF regulated expression of various genes. Its effects include down-regulation of cytokine, chemokine, cytokine receptor and proteinase expression. Down-regulation of IL-1R1, as well as inactivation of intracellular signaling pathways appeared to account for these effects. These collateral effects observed in the p21^{Cip1} gene transfer suggest new links between CDKIs and immunological effector molecules.

Acknowledgments

We thank Drs. T. Muneta, Y. Kuga, and J. Hasegawa for providing synovial samples; Drs. N. Terada and M. Ikeda for providing adenoviruses; Drs. R. Koike, H. Hagiyama, T. Nanki, and H. Nishitoh for their technical support and advice; and also Dr. N. Nishimura at Genetic Laboratory (Sapporo, Japan) performing DNA array experiments. We are grateful to Dr. T. Page for reviewing the manuscript.

References

1. Hale, L., and B. Haynes. 1997. Pathology of rheumatoid arthritis and associated disorders. In *Arthritis and Allied Conditions: A Textbook of Rheumatology*. W. Koopman, ed. Williams & Wilkins, Baltimore, p. 993.
2. Okada, Y. 2001. Proteinases and matrix degradation. In *Kelly's Textbook of Rheumatology*. Vol. 1. S. Ruddy, E. D. Harris, Jr., C. B. Sledge, eds. W. B. Saunders, Philadelphia. p. 55.
3. Taniguchi, K., H. Kohsaka, N. Inoue, Y. Terada, H. Ito, K. Hirokawa, and N. Miyasaka. 1999. Induction of the p16^{INK4a} senescence gene as a new therapeutic strategy for the treatment of rheumatoid arthritis. *Nat. Med. 5:760.*
4. Nasu, K., H. Kohsaka, Y. Nonomura, Y. Terada, H. Ito, K. Hirokawa, and N. Miyasaka. 2000. Adenoviral transfer of cyclin-dependent kinase inhibitor genes suppresses collagen-induced arthritis in mice. *J. Immunol. 165:7246.*
5. Nonomura, Y., H. Kohsaka, K. Nasu, Y. Terada, M. Ikeda, and N. Miyasaka. 2001. Suppression of arthritis by forced expression of cyclin-dependent kinase inhibitor p21^{Cip1} gene into the joints. *Int. Immunol. 13:723.*
6. Sherr, C. J., and J. M. Roberts. 1999. CDK inhibitors: positive and negative regulators of G_1-phase progression. *Genes Dev. 13:1501.*
7. Dotto, G. P. 2000. p21$^{WAF1/Cip1}$: more than a break to the cell cycle? *Acta Biochim. Biophys. 1471:M43.*
8. Arnett, F. C., S. M. Edworthy, D. A. Bloch, D. J. McShane, J. F. Fries, N. S. Cooper, L. A. Healey, S. R. Kaplan, M. H. Liang, and H. S. Luthra. 1988. The American Rheumatism Association 1987 revised criteria for the classification of rheumatoid arthritis. *Arthritis Rheum. 31:315.*
9. Terada, Y., T. Yamada, O. Nakashima, M. Tamamori, H. Ito, S. Sasaki, and F. Marumo. 1997. Overexpression of cell cycle inhibitors (p16^{INK4} and p21^{Cip1}) and cyclin D1 using adenovirus vectors regulates proliferation of rat mesangial cells. *J. Am. Soc. Nephrol. 8:51.*
10. Kumagai, T., T. Miki, M. Kikuchi, T. Fukuda, N. Miyasaka, R. Kamiyama, and S. Hirosawa. 1999. The proto-oncogene Bcl6 inhibits apoptotic cell death in differentiation-induced mouse myogenic cells. *Oncogene 18:467.*
11. Sadouk, M. B., J. P. Pelletier, G. Tardif, K. Kiansa, J. M. Cloutier, and J. Martel-Pelletier. 1995. Human synovial fibroblasts coexpress IL-1R type I and type II mRNA: the increased level of the IL-1 receptor in osteoarthritic cells is related to an increased level of the type I receptor. *Lab. Invest. 73:347.*
12. Moore, B. A., S. Aznavoorian, J. A. Engler, and L. J. Windsor. 2000. Induction of collagenase-3 (MMP-13) in rheumatoid arthritis synovial fibroblasts. *Acta Biochim. Biophys. 1502:307.*
13. Patel, R., B. Bartosch, and J. L. Blank. 1998. p21^{WAF1} is dynamically associated with JNK in human T lymphocytes during cell cycle progression. *J. Cell Sci. 111:2247.*
14. Renard, P., J. Ernest, A. Houbion, M. Art, H. Le Calvez, M. Raes, and J. Remacle. 2001. Development of a sensitive multi-well colorimetric assay for active NF-κB. *Nucleic Acids Res. 29:E21.*
15. Feldmann, M., F. M. Brennan, and R. N. Maini. 1996. Role of cytokines in rheumatoid arthritis. *Annu. Rev. Immunol. 14:397.*
16. Shim, J., H. Lee, J. Park, H. Kim, and E. J. Choi. 1996. A non-enzymatic p21 protein inhibitor of stress-activated protein kinases. *Nature 381:804.*
17. Bondeson, J., B. Foxwell, F. Brennan, and M. Feldmann. 1999. Defining therapeutic targets by using adenovirus: blocking NF-κB inhibits both inflammatory and destructive mechanisms in rheumatoid synovium but spares anti-inflammatory mediators. *Proc. Natl. Acad. Sci. USA 96:5668.*
18. Wendling, D., E. Racadot, and J. Wijdenes. 1993. Treatment of severe rheumatoid arthritis by anti-interleukin-6 monoclonal antibody. *J. Rheumatol. 20:259.*
19. Yoshizaki, K., N. Nishimoto, M. Mihara, and T. Kishimoto. 1998. Therapy of rheumatoid arthritis by blocking IL-6 signal transduction with a humanized anti-IL-6 receptor antibody. *Springer Semin. Immunopathol. 20:247.*
20. Koch, A. E., M. V. Volin, J. M. Woods, S. L. Kunkel, M. A. Connors, L. A. Harlow, D. C. Woodruff, M. D. Burdick, and R. M. Strieter. 2001. Regulation of angiogenesis by the C-X-C chemokines interleukin-8 and epithelial neutrophil activating peptide 78 in the rheumatoid joint. *Arthritis Rheum 44:31.*
21. Koch, A. E., S. L. Kunkel, L. A. Harlow, B. Johnson, H. L. Evanoff, G. K. Haines, M. D. Burdick, R. M. Pope, and R. M. Strieter. 1992. Enhanced production of monocyte chemoattractant protein-1 in rheumatoid arthritis. *J. Clin Invest. 90:772.*
22. Chabaud, M., G. Page, and P. Miossec. 2001. Enhancing effect of IL-1, IL-17, and TNF-α on macrophage inflammatory protein-3α production in rheumatoid arthritis: regulation by soluble receptors and Th2 cytokines. *J. Immunol. 167:6015.*
23. Gong, J. H., L. G. Ratkay, J. D. Waterfield, and I. Clark-Lewis. 1997. An antagonist of monocyte chemoattractant protein 1 (MCP-1) inhibits arthritis in the MRL-lpr mouse model. *J. Exp. Med. 186:131.*

24. Han, Z., D. L. Boyle, L. Chang, B. Bennett, M. Karin, L. Yang, A. M. Manning, and G. S. Firestein. 2001. c-Jun N-terminal kinase is required for metalloproteinase expression and joint destruction in inflammatory arthritis. *J. Clin. Invest. 108:73.*
25. Trabandt, A., R. E. Gay, H. G. Fassbender, and S. Gay. 1991. Cathepsin B in synovial cells at the site of joint destruction in rheumatoid arthritis. *Arthritis Rheum. 34:1444.*
26. Cunnane, G., O. FitzGerald, K. M. Hummel, R. E. Gay, S. Gay, and B. Bresnihan. 1999. Collagenase, cathepsin B and cathepsin L gene expression in the synovial membrane of patients with early inflammatory arthritis. *Rheumatology (Oxford) 38:34.*
27. Turk, B., D. Turk, and V. Turk. 2000. Lysosomal cysteine proteases: more than scavengers. *Acta Biochim. Biophys. 1477:98.*
28. Kaneko, M., T. Tomita, T. Nakase, Y. Ohsawa, H. Seki, E. Takeuchi, H. Takano, K. Shi, K. Takahi, E. Kominami, et al. 2001. Expression of proteinases and inflammatory cytokines in subchondral bone regions in the destructive joint of rheumatoid arthritis. *Rheumatology (Oxford) 40:247.*
29. Hou, W. S., W. Li, G. Keyszer, E. Weber, R. Levy, M. J. Klein, E. M. Gravallese, S. R. Goldring, and D. Bromme. 2002. Comparison of cathepsins K and S expression within the rheumatoid and osteoarthritic synovium. *Arthritis Rheum. 46:663.*
30. Dayer, J. M., U. Feige, C. K. Edwards III, and D. Burger. 2001. Anti-interleukin-1 therapy in rheumatic diseases. *Curr. Opin. Rheumatol. 13:170.*
31. Bresnihan, B., J. M. Alvaro-Gracia, M. Cobby, M. Doherty, Z. Domljan, P. Emery, G. Nuki, K. Pavelka, R. Rau, B. Rozman, et al. 1998. Treatment of rheumatoid arthritis with recombinant human interleukin-1 receptor antagonist. *Arthritis Rheum. 41:2196.*
32. Jiang, Y., H. K. Genant, I. Watt, M. Cobby, B. Bresnihan, R. Aitchison, and D. McCabe. 2000. A multicenter, double-blind, dose-ranging, randomized, placebo-controlled study of recombinant human IL-1 receptor antagonist in patients with rheumatoid arthritis: radiologic progression and correlation of Genant and Larsen scores. *Arthritis Rheum. 43:1001.*
33. Beutler, B. 2000. Tlr4: central component of the sole mammalian LPS sensor. *Curr. Opin. Immunol. 12:20.*
34. Fujisawa, K., H. Aono, T. Hasunuma, K. Yamamoto, S. Mita, and K. Nishioka. 1996. Activation of transcription factor NF-κB in human synovial cells in response to TNF-α. *Arthritis Rheum. 39:197.*
35. Asahara, H., K. Fujisawa, T. Kobata, T. Hasunuma, T. Maeda, M. Asanuma, N. Ogawa, H. Inoue, T. Sumida, and K. Nishioka. 1997. Direct evidence of high DNA binding activity of transcription factor AP-1 in rheumatoid arthritis synovium. *Arthritis Rheum. 40:912.*
36. Han, Z., D. L. Boyle, A. M. Manning, and G. S. Firestein. 1998. AP-1 and NF-κB regulation in rheumatoid arthritis and murine collagen-induced arthritis. *Autoimmunity 28:197.*
37. Aupperle, K. R., B. L. Bennett, D. L. Boyle, P. P. Tak, A. M. Manning, and G. S. Firestein. 1999. NF-κB regulation by IκB kinase in primary fibroblast-like synoviocytes. *J. Immunol. 163:427.*
38. Georganas, C., H. Liu, H. Perlman, A. Hoffmann, B. Thimmapaya, and R. M. Pope. 2000. Regulation of IL-6 and IL-8 expression in rheumatoid arthritis synovial fibroblasts: the dominant role for NF-κB but not C/EBPβ or c-Jun. *J. Immunol. 165:7199.*
39. Mengshol, J. A., K. S. Mix, and C. E. Brinckerhoff. 2002. Matrix metalloproteinases as therapeutic targets in arthritic diseases: bull's-eye or missing the mark? *Arthritis Rheum. 46:13.*
40. Auron, P. E., and A. C. Webb. 1994. Interleukin-1: a gene expression system regulated at multiple levels. *Eur. Cytokine Netw. 5:573.*
41. Roebuck, K. A. 1999. Regulation of interleukin-8 gene expression. *J. Interferon Cytokine Res. 19:429.*
42. Gelb, B. D., G. P. Shi, M. Heller, S. Weremowicz, C. Morton, R. J. Desnick, and H. A. Chapman. 1997. Structure and chromosomal assignment of the human cathepsin K gene. *Genomics 41:258.*
43. Lucio-Cazana, J., K. Nakayama, Q. Xu, T. Konta, V. Moreno-Manzano, A. Furusu, and M. Kitamura. 2001. Suppression of constitutive but not IL-1β-inducible expression of monocyte chemoattractant protein-1 in mesangial cells by retinoic acids: intervention in the AP-1 pathway. *J. Am. Soc. Nephrol. 12:688.*
44. Ye, K., C. A. Dinarello, and B. D. Clark. 1993. Identification of the promoter region of human interleukin-1 type I receptor gene: multiple initiation sites, high G+C content, and constitutive expression. *Proc. Natl. Acad. Sci. USA 90:2295.*
45. Spiegelman, V. S., P. Stavropoulos, E. Latres, M. Pagano, Z. Ronai, T. J. Slaga, and S. Y. Fuchs. 2001. Induction of β-transducin repeat-containing protein by JNK signaling and its role in the activation of NF-κB. *J. Biol. Chem. 276:27152.*
46. Das, K. C. 2001. c-Jun NH_2-terminal kinase-mediated redox-dependent degradation of IκB: role of thioredoxin in NF-κB activation. *J. Biol. Chem. 276:4662.*
47. Chang, B. D., K. Watanabe, E. V. Broude, J. Fang, J. C. Poole, T. V. Kalinichenko, and I. B. Roninson. 2000. Effects of p21$^{Waf1/Cip1/Sdi1}$ on cellular gene expression: implications for carcinogenesis, senescence, and age-related diseases. *Proc. Natl. Acad. Sci. USA 97:4291.*
48. DiPaolo, B. R., R. J. Pignolo, and V. J. Cristofalo. 1992. Overexpression of the two-chain form of cathepsin B in senescent WI-38 cells. *Exp. Cell Res. 201:500.*

Amelioration of Collagen-Induced Arthritis by Blockade of Inducible Costimulator-B7 Homologous Protein Costimulation[1]

Hideyuki Iwai,*† Yuko Kozono,* Sachiko Hirose,‡ Hisaya Akiba,§ Hideo Yagita,§ Ko Okumura,§ Hitoshi Kohsaka,† Nobuyuki Miyasaka,† and Miyuki Azuma[2]*

B7 homologous protein (B7h)/B7-related protein 1 (B7RP-1) is a new member of the B7 family of costimulatory molecules that specifically interacts with inducible costimulator (ICOS) expressed on activated T cells. Collagen type II (CII)-induced arthritis (CIA) is an experimental model of arthritis that has been used to dissect the pathogenesis of human rheumatoid arthritis. In this study, we have investigated the effect of neutralizing anti-B7h mAb on the development and disease progression of CIA. Administration of anti-B7h mAb significantly ameliorated the disease as assessed by clinical arthritis score and histology in the joints, and a beneficial effect was also obtained by a delayed treatment after the onset of disease. Expression of ICOS and B7h was observed in the inflamed synovial tissue as well as in the draining lymph nodes (LNs) and expansion of ICOS$^+$ T cells in the LN was reduced by the anti-B7h mAb treatment. Expression of mRNA for proinflammatory cytokines such as TNF-α, IL-1β, and IL-6 in the joints was inhibited by the treatment. Proliferative responses and production of IFN-γ and IL-10 upon restimulation with CII in vitro were significantly inhibited in LN cells from the anti-B7h mAb-treated mice. Serum anti-CII IgG1, IgG2a, and IgG2b levels were also reduced. Our present results showed a beneficial effect of the B7h blockade on CIA through anti-inflammatory actions and inhibition of both Th1- and Th2-mediated immune responses, suggesting that the ICOS-B7h interaction plays an important role in the pathogenesis of CIA and thus the blockade of this pathway may be beneficial for the treatment of human rheumatoid arthritis. ***The Journal of Immunology,*** **2002, 169: 4332–4339.**

Successful T cell activation requires the engagement of the TCR with Ag/MHC as well as the engagement of costimulatory molecules provided by the cognate interactions of T cells with APCs (1, 2). CD28 is a most extensively characterized costimulatory molecule on T cells and interacts with CD80 and CD86 on APCs. CD28 is expressed on most naive T cells and the CD28 costimulatory pathway plays a particularly critical role in the initial activation of naive T cells. Blockade of CD28 pathway has been shown to ameliorate experimental autoimmune diseases such as lupus, experimental autoimmune encephalomyelitis (EAE),[3] diabetes, and arthritis (3–6).

Recently, new members of the CD28-B7 family have been identified. The inducible costimulator (ICOS) is one of such molecules expressed on activated T cells (7–10). The ICOS ligand, B7 homologous protein (B7h) (11)/B7-related protein 1 (B7RP-1) (12)/GL50 (13)/ligand of ICOS (14), hereafter designated B7h, is constitutively expressed on B cells and is inducible on monocytes and dendritic cells at low levels (15, 16). B7h expression in these APCs and fibroblasts could be induced by proinflammatory cytokines such as IFN-γ and TNF-α (11). Ligation of ICOS on activated T cells by mAb or B7h fusion proteins strongly enhanced the production of multiple cytokines including IL-4, IL-5, IFN-γ, and IL-10, whereas IL-2 production was not clearly enhanced (7, 15, 17). These results suggested a unique property of the ICOS-mediated costimulation distinct from the CD28-mediated costimulation. Earlier studies of the ICOS blockade (10, 18) and ICOS-deficient mice (19–21) suggested a predominant role of the ICOS costimulation in Th2-mediated humoral immune responses. However, recent studies also demonstrated the involvement of ICOS in Th1- and CD8$^+$ T cell-mediated cellular immune responses (22–25). Another intriguing feature of the ICOS blockade distinct from the CD28 blockade is the fact that the ICOS blockade was effective at the efferent phase, but not at the induction phase of both Th1- and Th2-mediated responses (26, 27). These results suggest that ICOS may be a potent costimulator for effector T cells.

The collagen-induced arthritis (CIA) model has been extensively used to elucidate pathogenic mechanisms relevant to human rheumatoid arthritis and to identify potential targets for therapeutic intervention (28). A murine model of CIA can be induced in genetically susceptible mice such as DBA/1 by intradermal injection of type II collagen (CII) in adjuvant. The development of CIA is known to be dependent on CD4$^+$ T cell activation and Ab production against CII (28). In addition to these Ag-specific immune responses, local production of proinflammatory cytokines, such as TNF-α, IL-1β, and IL-6, is involved in the pathogenesis of CIA (29). In this study, we have examined the effects of the administration of mAb against B7h in the murine CIA model and investigated the involvement of the ICOS-B7h costimulatory pathway in the development and disease progression of CIA.

Departments of *Molecular Immunology and †Bioregulatory Medicine and Rheumatology, Graduate School, Tokyo Medical and Dental University, Tokyo, Japan; and Departments of ‡Pathology and §Immunology, Juntendo University School of Medicine, Tokyo, Japan

Received for publication January 23, 2002. Accepted for publication August 12, 2002.

The costs of publication of this article were defrayed in part by the payment of page charges. This article must therefore be hereby marked *advertisement* in accordance with 18 U.S.C. Section 1734 solely to indicate this fact.

[1] This work was supported in part by a Grant-in-Aid for Scientific Research from the ministry of Education, Culture, Sports, Science and Technology and from the Ministry of Health, Labor, and Welfare of Japan.

[2] Address correspondence and reprint requests to Dr. Miyuki Azuma, Department of Molecular Immunology, Division of Oral Health Sciences, Graduate School, Tokyo Medical and Dental University, 1-5-45 Yushima, Bunkyo-ku, Tokyo 113-8549, Japan. E-mail address: miyuki.mim@tmd.ac.jp

[3] Abbreviations used in this paper: EAE, experimental autoimmune encephalomyelitis; ICOS, inducible costimulator; B7h, B7 homologous protein; B7RP-1, B7-related protein 1; CIA, collagen-induced arthritis; CII, collagen type II; LN, lymph node; dCII, denatured CII.

0022-1767/02/$02.00

Materials and Methods

Mice

Specific pathogen-free 6-wk-old male DBA/1J mice were purchased from the Japan Charles River Breeding Laboratories (Kanagawa, Japan) and maintained in the animal facility at the Tokyo Medical and Dental University (Tokyo, Japan). All mice procedures were reviewed and approved by the Animal Care and Use Committee in the Tokyo Medical and Dental University.

Ig fusion protein, transfectants, mAbs, and immunofluorescence

The Ig fusion protein consisting of the extracellular portion of mouse ICOS (aa 1–147) (30) linked to the Fc portion of human IgG1 (ICOS-Ig) and OX40-Ig were prepared as described previously (31). Mouse B7h cDNA was generated by RT-PCR from peritoneal macrophages of BALB/c mice and was subsequently subcloned into a pMKITneo vector (kindly provided by Dr. K. Maruyama, Tokyo Medical and Dental University). Primers used to generate a full-length B7h cDNA were: sense, 5′-GACGAATTCATG CAGCTAAAGTGTCCCTG-3′ including an *Eco*RI cloning site; and antisense, 5′-GACCTCGAGTCAGGCGTGGTCTGTAAGTT-3′ including a *Xho*I cloning site. NRK-52E (NRK) and L cells were transfected with a B7h/pMKITneo expression vector by electroporation, drug selected, and cells expressing B7h were identified by staining with ICOS-Ig. The anti-mouse B7h mAb (HK5.3, rat IgG2a) was generated by immunizing SD rats with mouse B7h-transfected L cells and fusing immune splenocytes with P3U1 myeloma cells and screened for binding to mouse B7h-transfected NRK cells.

For in vitro blocking experiments, anti-mouse CD80 (RM80, rat IgG2a) (32), CD86 (PO3, rat IgG2b) (32), CD154 (MR1, hamster IgG) (33), and CD134L (RM134L, rat IgG2b) (34) mAbs were used. All mAbs were purified from ascites as described previously (3, 32). Rat IgG (Sigma-Aldrich, St. Louis, MO) was used as a control reagent. For immunofluorescent analysis, PerCP-conjugated anti-CD3 mAb (145-2C11, hamster IgG) and FITC-conjugated anti-ICOS mAb (B10.5, rat IgG2a, kindly provided by JT Central Pharmaceutical Research Institute, Osaka, Japan) (35), or appropriate fluorochrome-conjugated control Ig were used. All fluorochrome-conjugated mAbs and control Ig were obtained from BD PharMingen (San Diego, CA), unless otherwise noted. For indirect staining, PE-conjugated anti-human IgG (Caltag Laboratories, Burlingame, CA) and PE-conjugated anti-rat IgG (Caltag Laboratories) were used for the second-step Abs. Immunofluorescence, flow cytometry, and data analysis were performed using FACSCalibur and CellQuest software (BD Biosciences, San Jose, CA).

Induction of CIA, Ab treatment, and clinical assessment of arthritis

CIA was induced as previously described with minor modifications (36). Briefly, male DBA/1J mice (7–10 wk old) were injected intradermally at the base of the tail with 200 μg of bovine CII (Collagen Research Center, Tokyo, Japan) in 0.05 M acetic acid, emulsified in CFA (Difco, Detroit, MI). Twenty-one days after primary immunization, the mice were boosted in the same way. The day of second immunization (booster) was designated as day 0. The immunized mice were randomly divided and treated with the following regimens. Each group of mice received either control IgG or anti-B7h mAb (50, 100, or 300 μg/body) i.p. on days −1, 1, 3, and 5. In our preliminary experiment, we have observed no obvious differences between the mice treated with three doses of control IgG. We therefore selected a single dose, 100 μg/body for a control group. In the experiments for a delayed treatment, 100 μg/body control IgG or anti-B7h mAb was injected i.p. on days 5, 7, 9, and 11. Mice were examined daily for the onset of CIA. The swelling of four paws was graded from 0 to 4 as follows: grade 0, no swelling; grade 1, swelling of finger joints or focal redness; grade 2, mild swelling of wrist or ankle joints; grade 3, severe swelling of the entire paw; and grade 4, deformity or ankylosis. Each paw was graded, and the four scores were totaled so that the maximal score per mouse was 16. Incidence was expressed as the number of mice that showed paw swelling in the total number of mice examined, and the time of onset was expressed as the mean time when paw swelling was first observed in individual mice.

Histological and radiological assessments of arthritis

CIA mice were killed at day 35. Anteroposterior radiographs of the four limbs were obtained with a cabinet soft x-ray apparatus (CMB-2; Softex, Tokyo, Japan). Then, the hind paws were removed, fixed in Formalin, decalcified in 10% EDTA, embedded in paraffin, sectioned, and stained with H&E.

ICOS, B7h, and proinflammatory cytokine expression in the synovium

In some experiments, the knee joints from CIA mice at day 5 were removed and subjected to immunohistological analysis. Cryostat sections were fixed in acetone and 1% paraformaldehyde. For detection of ICOS, the sections were stained with biotinylated anti-ICOS mAb (B10.5) followed by biotinylated rabbit anti-rat IgG Ab (DAKO-Japan, Kyoto, Japan), Alexa 488-conjugated streptavidin (Molecular Probes, Eugene, OR), normal rat serum for blocking, and then Alexa 594-conjugated rat anti-CD4 (GK1.5) mAb.

For detection of B7h, the sections were stained with biotinylated ICOS-Ig and then HRP-conjugated streptavidin followed by Alexa 488-tyramide (TSA kit 22; Molecular Probes). After blocking with normal rat serum, Alexa 594-conjugated rat anti-CD45R (B220) was further stained. Conjugation of Alexa 594 to anti-CD45R and CD4 mAbs were performed using a Alexa Fluor 594 protein labeling kit (Molecular Probes) according to the protocols recommended by the manufacturer. The staining profiles were obtained with a fluorescence microscope (Olympus BX-50; Olympus, Tokyo, Japan) equipped with a charge-coupled device camera (PXL System; Photometrics, Tucson, AZ) and the image was analyzed by using IPLab Spectrum software (Signal Analytics, Vienna, VA).

For RT-PCR analysis, synovial tissues were isolated from the knee joints, and total RNA was extracted by using Concert cytoplasmic RNA reagent (Invitrogen, Tokyo, Japan). First-strand cDNA was synthesized using oligo(dT) primer and Superscript II reverse transcriptase (Life Technologies, Gaithersburg, MD). PCR was performed using the following primers: mouse TNF-α (sense, 5′-GCCACCACGCTCTTCTG-3′ and antisense, 5′-ATGGGCTCATACCAGGG-3′); mouse IL-1β (sense, 5′-CT GAAAGCTCTCCACCTC-3′ and antisense, 5′-GGTGCTGATGTACCA GTTG-3′); mouse IL-6 (sense, 5′-TCCTCTCTGCAAGAGACTT-3′ and antisense, 5′-TTCTGCAAGTGCATCATCG-3′); mouse ICOS (sense, 5′-GTACTTCTGCCATGTCTTTG-3′ and antisense, 5′-TGAGGTCACACC TGCAAGT-3′); mouse B7h (sense, 5′-GTGTCCCTGTTTTGTGTCC-3′ and antisense, 5′-TGAAGTTTGCTGCCACACG-3′); and mouse GAPDH (sense, 5′-GCCAAACGGGTCATCATCTC-3′ and antisense, 5′-GACA CATTGGGGGTAGGAAC-3′). For quantification of the PCR products, the amounts of cDNA were preliminarily normalized to produce the same amount of PCR products for GAPDH based on the intensity of the ethidium bromide staining of each band measured by the charge-coupled device imaging system (Densitograph AE-6920 M; Atto, Tokyo, Japan). The cDNA samples from four individual mice in each group were amplified on a DNA thermal cycler (PerkinElmer, Norwalk, CT) for 30 cycles except for 25 cycles of GAPDH. The PCR condition was as follows: 94°C for 1 min, followed by 58°C (cytokines and GAPDH), 55°C (ICOS), or 56°C (B7h) for 1 min, and 72°C for 2 min with a 15-min extension at 72°C at the end. The PCR products were electrophoresed on agarose gel, stained with ethidium bromide, and the image was acquired using the Densitograph.

CII-specific T cell proliferation and cytokine production

Five days or 10 wk after the second immunization, draining lymph nodes (LNs) and the spleen were removed. Single-cell suspensions of LN cells and erythrocyte-depleted splenocytes were prepared in RPMI 1640 medium supplemented with 10% FBS, 2 mM glutamine, 1 mM sodium pyruvate, 5×10^{-5} M 2-ME, and antibiotics. For purification of $CD4^+$ T cells, cells were treated with anti-I-A, anti-CD24, anti-CD45R, and anti-CD8 mAbs and rabbit complement and the purity of $CD4^+$ T cells was confirmed to be >95% $CD4^+$ cells by flow cytometry. Whole splenocytes, LN cells (5×10^5/well), or $CD4^+$ splenic T cells (2.5×10^5/well) were seeded in 96-well flat-bottom microtiter plates and cultured in the presence or absence of the indicated amounts of denatured (60°C, 30 min) bovine CII (dCII) for 72 h. In the culture with purified $CD4^+$ T cells, splenocytes from the mice at 5 days after the second immunization were treated with mitomycin C (50 μg/ml, 37°C, 30 min; Sigma-Aldrich) and the cells (2.5×10^5/well) were added as APCs. For in vitro mAb blocking experiments, LN cells from the mice 8 wk after the primary immunization were used and cultured as described above. The blocking mAb was added at the start of the assay. All cultures were pulsed with [^{3}H]thymidine (0.5 μCi/well; DuPont NEN, Boston, MA) for the last 16 h, harvested on a Micro 96 Harvester (Skatron, Lier, Norway), and the incorporated radioactivity was measured using a microplate beta counter (Micro Beta Plus; Wallac, Turku, Finland). Supernatants from similar cultures were collected after 96 h for the assessment of cytokine production by ELISA. ELISA for mouse IFN-γ, IL-4, and IL-10 was performed using ELISA kits (Ready-SET-Go!; eBioscience, San Diego, CA) according to the protocols recommended by the manufacturer.

Serum anti-CII Ab levels

Serum samples were collected on days 7, 14, and 21, and the titers of anti-CII IgG Abs were measured by ELISA. Bovine CII (1 μg/ml) was coated onto microtiter plates (Maxisorp; Nunc, Roskilde, Denmark) overnight at 4°C. After blocking with 1% BSA in PBS, serially diluted serum samples were added and incubated for 1 h at room temperature. After washing, HRP-conjugated rabbit anti-mouse IgG1, IgG2a, or IgG2b Ab (Zymed Laboratories, San Francisco, CA) was added and incubated for 2 h at 37°C. After washing, Ab binding was visualized using *o*-phenylenediamine (Sigma-Aldrich). A standard serum composed of a mixture of sera from arthritic mice was added to each plate in serial dilutions and a standard curve was constructed. The standard serum was defined as 1 U and the Ab titers of serum samples were determined by the standard curve.

Statistical analysis

Significant differences between experimental groups were analyzed by the Mann-Whitney *U* test. Values of $p < 0.05$ were considered to be significant.

Results

Inhibitory effect of anti-B7h mAb on CII-specific T cell proliferative responses in vitro

We generated a mAb (HK5.3) against mouse B7h by immunizing SD rats with B7h transfectants. Similar to the staining with ICOS-Ig, HK5.3 specifically bound to B7h-transfected NRK (B7h/NRK) cells, but not to parental NRK cells (Fig. 1*A*). Preincubation with HK5.3, but not with control rat IgG (data not shown) efficiently blocked the ICOS-Ig binding to B7h/NRK cells, indicating the specific binding of HK5.3 to the ICOS ligand B7h. To evaluate the functional inhibitory effects of this anti-B7h mAb, we examined the effect of this mAb on CII-specific proliferative responses in vitro. LN cells from CII-immunized mice were stimulated with 30 μg/ml dCII and a panel of mAbs against costimulatory molecules (Fig. 1*B*) and the titrated amount of anti-B7h mAb (Fig. 1*C*) was added to the culture. The addition of dCII dramatically enhanced proliferative responses and this enhanced proliferation was clearly inhibited by anti-B7h mAb as well as by anti-CD80 and CD86 mAbs, anti-CD134L mAb, or anti-CD154 mAb. The inhibitory effect of anti-B7h mAb occurred in a dose-dependent manner. These results indicate an inhibitory activity of anti-B7h mAb and a substantial involvement of B7h in the CII-specific T cell responses in vitro.

Preventive and therapeutic effects of anti-B7h mAb on CIA

To investigate the role of ICOS-B7h-mediated T cell costimulation in the development of autoimmune arthritis, we examined the effects of anti-B7h mAb on the development of CIA. DBA/1J mice were immunized twice with bovine CII in CFA to elicit CIA. Four groups of mice were i.p. administrated either 50, 100, and 300 μg of anti-B7h mAb or 100 μg of control IgG every other day from day −1 for four times. As shown in Fig. 2*A*, the mice treated with control IgG developed severe arthritis. In contrast, the administration of anti-B7h mAb significantly ameliorated the clinical manifestations of CIA in a dose-dependent manner. As summarized in Table I, the treatment with 100 μg of anti-B7h mAb significantly delayed the day of onset and decreased the mean arthritis score and the mean number of arthritic paws, although the incidence of disease was not affected. The amelioration of clinical arthritis by the anti-B7h mAb treatment was confirmed by histopathological examination of the joints. The hind paw sections from the control IgG-treated mice at day 35 showed infiltration of mononuclear cells, synovial hyperplasia, pannus formation, cartilage destruction, and bone erosion that are characteristic features of arthritis (Fig. 3*c*). These features were clearly ameliorated by the anti-B7h mAb treatment (Fig. 3*d*). Radiological examination also showed

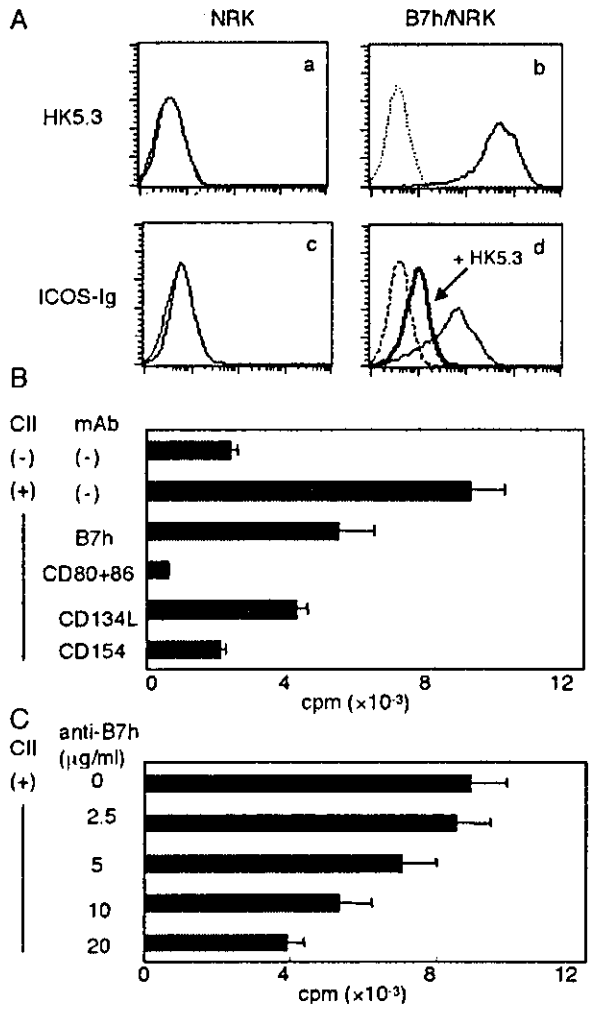

FIGURE 1. Characterization of anti-B7h mAb (HK5.3). *A*, Specific binding of HK5.3 to mouse B7h. NRK (*a* and *c*) and B7h/NRK (*b* and *d*) cells were stained with HK5.3 (*a* and *b*) and ICOS-Ig (*c* and *d*) followed by PE-anti-rat IgG and PE-anti-human IgG Abs, respectively. Samples were analyzed by flow cytometry. Histograms from the cells stained with control Ig (rat IgG2a) or fusion protein (OX40L-Ig) are overlayed. The bold line in *d* shows a histogram of the cells preincubated with HK5.3 before staining with ICOS-Ig. Preincubation with control rat IgG2a did not inhibit the binding of ICOS-Ig to B7h/NRK cells (data not shown). *B* and *C*, Inhibitory effects on CII-specific proliferative responses. LN cells from the CII-immunized mice were restimulated with or without 30 μg/ml dCII in the presence or absence of the indicated mAbs. Cultures were pulsed with [^{3}H]thymidine for the last 16 h of a 72-h culture and the incorporated radioactivity was measured. All mAbs were used at a final concentration of 10 μg/ml (*B*) or anti-B7h mAb was used at the indicated concentrations (*C*). Data are expressed as the mean ± SEM of triplicate cultures. The data shown are representative of two independent experiments with similar results.

the prevention of bone erosion by the anti-B7h mAb treatment (Fig. 3, *a* and *b*).

To investigate whether the treatment with anti-B7h mAb is still effective after the onset of disease, we have performed a delayed treatment. Since day 5 was the mean day of onset in the control IgG-treated mice as shown in Table I, we started a similar treatment from day 5 and examined the clinical scores. The delayed treatment was also effective in reducing the clinical arthritis scores (Fig. 2*B*). These results demonstrated that the treatment with anti-B7h mAb either before or after the onset of disease could inhibit

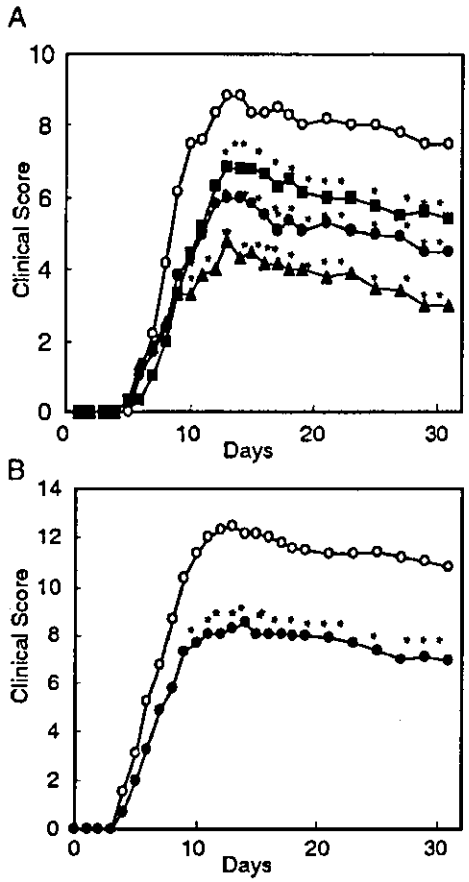

FIGURE 2. Effect of anti-B7h mAb treatment on clinical scores. CIA was induced by primary (day −21) and secondary (day 0) immunization with bovine type II collagen in CFA. *A*, Four groups of mice were injected i.p. with either 100 μg of control IgG (○) or 50 (■), 100 (●), or 300 (▲) μg of anti-B7h mAb on days −1, 1, 3, and 5. *B*, Two groups of mice were injected i.p. with 100 μg of control IgG (○) or anti-B7h mAb (●) on days 5, 7, 9, and 11. Data are expressed as the mean of seven mice in each group. The data shown are representative of three independent experiments with similar results. *, Statistically different from the control IgG-treated group ($p < 0.05$).

the disease severity of CIA, suggesting the involvement of the ICOS-B7h pathway in the pathogenesis.

Expression of ICOS and B7h in the joints and the draining LNs

To determine the expression of ICOS and B7h in the inflamed joints and the draining LN cells, immunohistological staining and flow cytometry were performed using a specific mAb against ICOS and B7h or ICOS-Ig. ICOS expression was observed on both $CD4^+$ and $CD4^-$ (presumably $CD8^+$ T) cells in the synovium of the inflamed joints from the control IgG-treated mice on day 5 (Fig. 4*Ab*). We first performed immunohistological staining using anti-B7h mAb; however, the positive staining was not observed even in the spleen and LN as well as in the synovial tissue, suggesting that this anti-B7h mAb (HK5.3) is not applicable to immunohistological staining. We therefore used ICOS-Ig for detection of B7h expression. Positive cells were observed within some of the $CD45R^+$ B cells (Fig. 4*Ac*) and $CD11b^+$ macrophages, and then weakly on $CD11c^+$ dendritic cells (data not shown) in the inflamed joints. To further assess the change of ICOS and B7h expression in the inflamed joints, the mRNA levels for ICOS and B7h were compared between naive and the control IgG-treated CIA mice. The mRNA expression for ICOS and B7h in the joints

Table I. *Effect of anti-B7h mAb treatment on CIA*[a]

	Control IgG	Anti-B7h mAb
Day of onset	4.9 ± 1.3	6.3 ± 2.9[b]
Clinical score (day 12)	11.8 ± 3.6	6.3 ± 3.8[b]
Arthritic paw (day 12)	3.0 ± 0.9	2.4 ± 1.0[b]
Incidence (day 12)	24/26 (92%)	24/26 (92%)

[a] CIA was induced as described in Fig. 2 and treated with either 100 μg of control IgG or anti-B7h mAb on days −1, 1, 3, and 5. Values represent the mean ± SD from each group of 26 mice.
[b] Statistically different from the control IgG-treated group ($p < 0.05$).

was significantly enhanced in the CIA mice (Fig. 4*B*). We next investigated draining LN cells. The mean total number of LN cells in the control IgG-treated CIA mice ($2.5 \pm 0.1 \times 10^7$ cells) was clearly enhanced as compared with that in the naive mice and this enhancement was reduced in the anti-B7h mAb-treated mice ($1.6 \pm 0.3 \times 10^7$ cells). However, the ratio of T ($CD3^+$), B ($CD45R^+CD3^-$), or non-T/B ($CD3^-CD45R^-$) LN cells was not affected by the anti-B7h mAb treatment (data not shown). $ICOS^+$ T cells were clearly increased in the control IgG-treated CIA mice (8.2 ± 1.0%) as compared with naive mice (4.9 ± 0.3%; data not shown), but this increase was significantly inhibited in the anti-B7h mAb-treated mice (5.3 ± 0.3%; Fig. 4*C*). Consistent with a previous report (15), a constitutive expression of B7h was observed on B cells in naive mice and this expression on LN-B cells was not clearly affected by the CII immunization and the anti-B7h mAb treatment (data not shown). These results demonstrated a substantial expression of ICOS and B7h in the local joints as well as in the draining LNs in CIA mice.

Down-regulation of proinflammatory cytokines in the joints by anti-B7h mAb treatment

Since the inflammatory process in the synovium plays a major role in the development of arthritis (29), we next examined the change of proinflammatory cytokine expression in the synovium by the treatment. Consistent with previous reports (29, 37), high levels of TNF-α, IL-1β, and IL-6 mRNA were observed in the synovial tissues from the control IgG-treated mice, but the treatment with anti-B7h mAb significantly inhibited the expression of these proinflammatory cytokines (Fig. 5). These results suggested that the

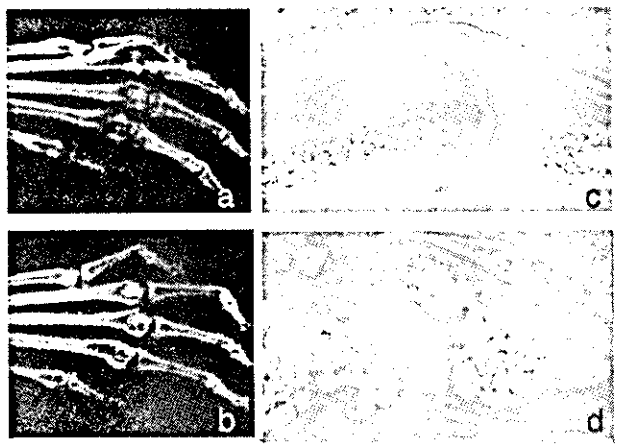

FIGURE 3. Effect of anti-B7h mAb treatment on histopathological arthritis. Hind paws from the control IgG-treated (*a* and *c*) or anti-B7h-treated (*b* and *d*) CIA mice at day 35 were examined by soft x-ray radiograph (*a* and *b*) and H&E staining of the metatarsophalangeal joints (*c* and *d*). Original magnification, ×100. Representative radiograph and staining from each group of seven mice are shown.

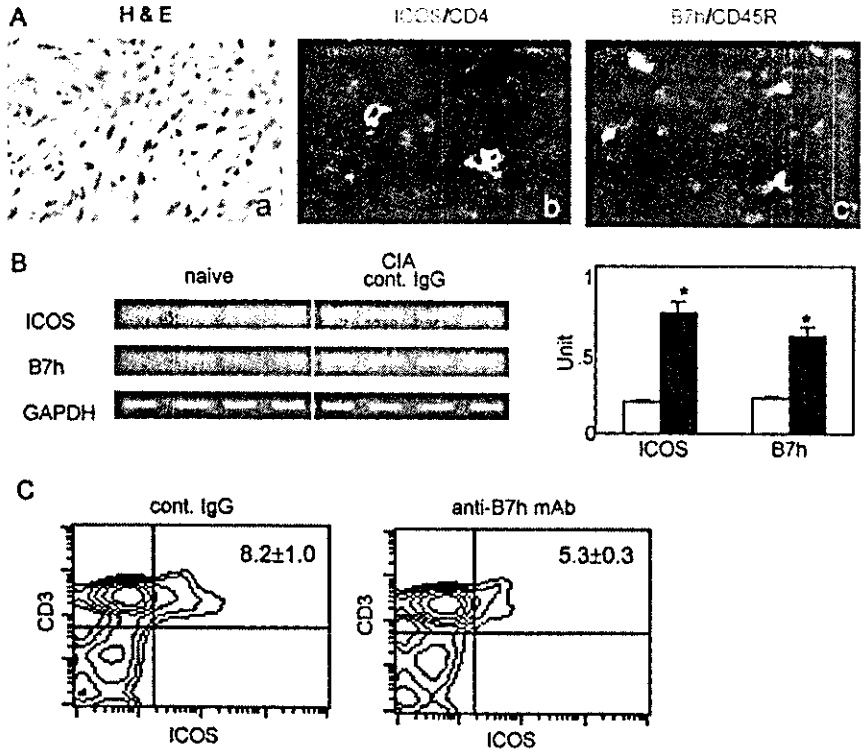

FIGURE 4. Expression of ICOS and B7h in the joints and draining LNs. *A*, The cryostat sections of hind paws from the control IgG-treated CIA mice at day 5 were stained with H&E (*a*), a combination of anti-CD4 (red fluorescence) and anti-ICOS (green fluorescence) mAbs (*b*), or anti-CD45R mAb (red fluorescence) and ICOS-Ig (green fluorescence, *c*). Representative regions of the synovium are shown. Yellow stains show $ICOS^+CD4^+$ or $B7h^+CD45R^+$ cells. Original magnification, ×400. *B*, The joints of hind paws from naive mice and the control IgG-treated mice at day 5 were removed and mRNA expression for ICOS and B7h was assessed by RT-PCR. Data represent four individual mice from each group. The expected product sizes for ICOS, B7h, and GAPDH are 592, 482, and 379 bp, respectively. Data represent four individual mice from each group. The amount of mRNA was measured by densitography and the unit values were normalized to the amount of mRNA for GAPDH. The mean ± SEM of unit values in naive (□) and the control IgG-treated CIA (■) mice are shown. *, Statistically different from naive mice ($p < 0.05$). *C*, LN cells from CIA mice treated with control IgG or anti-B7h mAb were stained with FITC-conjugated anti-ICOS mAb and PerCP-conjugated anti-CD3 mAb or with appropriate fluorochrome-conjugated control Ig, and samples were analyzed by flow cytometry. Representative data from three mice are displayed as contour plots (4-decade log scale) and the quadrant markers have been positioned to include >98% of control Ig-stained cells (data not shown) in the *lower left*. The mean percentage ± SEM for $ICOS^+CD3^+$ cells from three mice in each group are indicated in the *upper right* of each panel.

anti-B7h mAb treatment reduced the arthritic manifestations by down-regulating the expression of proinflammatory cytokines in the joints.

Inhibition of CII-specific T cell proliferation and cytokine production by anti-B7h mAb treatment

The intervention of the ICOS-B7h costimulatory pathway by anti-B7h mAb might modulate CII-specific T cell responses and might affect the Th1/Th2 balance. To address these possibilities, splenocytes and LN cells at day 5 were isolated from the CIA mice, and proliferative responses and cytokine production against CII were examined. Splenocytes from the control IgG-treated mice proliferated well in response to dCII, whereas splenocytes from naive mice did not proliferate even at a high concentration of dCII (Fig. 6*Aa*). Splenocytes from the anti-B7h mAb-treated mice showed significantly reduced proliferative responses to dCII as compared with those from the control IgG-treated mice. A similar inhibitory effect of the anti-B7h mAb treatment was observed when $CD4^+$ splenic T cells (Fig. 6*Ab*) or LN cells (Fig. 6*Ac*) were used as responder cells. These results suggested that the anti-B7h mAb treatment at the second immunization inhibited the expansion of CII-specific T cells in the LN and spleen. We next examined the Th1 and Th2 cytokine production. LN cells from the control IgG- or anti-B7h mAb-treated mice were stimulated with 30 μg/ml dCII for 96 h, and IFN-γ, IL-4, and IL-10 in the supernatants were measured by ELISA. LN cells from the control IgG-treated mice produced high levels of IFN-γ and IL-10 in response to CII, but the production of these cytokines by LN cells was greatly reduced in the anti-B7h mAb-treated mice (Fig. 6*B*). IL-4 production was undetectable in both groups of mice in this culture condition (data not shown). Inhibitory effect by the anti-B7h mAb treatment on IFN-γ production was persistently observed even at 10 wk after the second immunization (Fig. 6*C*). These results suggested that the anti-B7h mAb treatment prevented the differentiation and/or expansion of CII-specific Th1 and Th2 cells and prolonged the inhibitory effect on Th1-mediated responses.

Inhibition of anti-CII IgG1, IgG2a, and IgG2b Ab production by anti-B7h mAb treatment

It is well known that IgG2a production is mainly induced by the Th1 cytokine IFN-γ and other IgG isotypes are regulated by Th2 cytokines such as IL-4, IL-5, IL-6, and IL-10 (38, 39). We thus investigated the anti-CII IgG1, IgG2a, and IgG2b Ab levels in the sera from the control IgG- or anti-B7h mAb-treated mice at 7, 14, and 21 days after the second immunization. The serum levels of anti-CII IgG1, IgG2a, and IgG2b were dramatically increased in response to the second immunization, but all of these responses were significantly suppressed by the anti-B7h mAb treatment (Fig. 7). These results indicated that the anti-B7h mAb treatment inhibited the production of anti-CII Abs that is dependent on either Th1

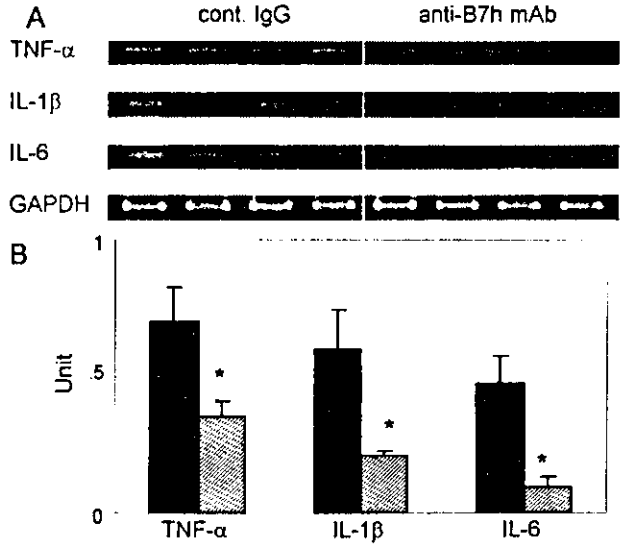

FIGURE 5. Expression of proinflammatory cytokines in the joints. *A*, The joints of hind paws from control IgG- or anti-B7h mAb-treated mice at day 5 were removed and mRNA expression for TNF-α, IL-1β, and IL-6 was assessed by RT-PCR. The expected product sizes for TNF-α, IL-1β, and IL-6 are 452, 297, and 248 bp, respectively. Data represent four individual mice from each group. *B*, The unit values were measured as described in Fig. 4 and the mean ± SEM of unit values from four control IgG (■)- and anti-B7h mAb (▨)-treated mice are shown. Similar results were obtained in three independent experiments. *, Statistically different from the control IgG-treated group ($p < 0.05$).

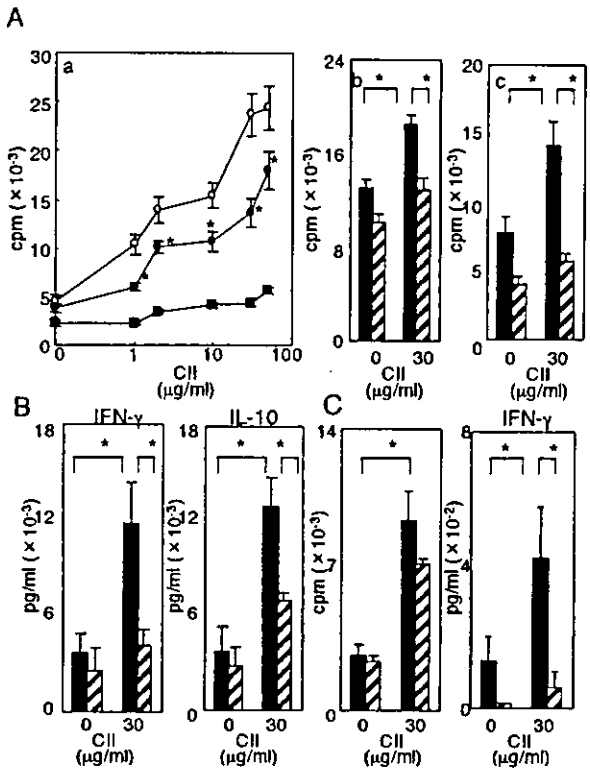

FIGURE 6. Effects of anti-B7h mAb treatment on CII-specific T cell proliferation and cytokine production. *A*, Whole splenocytes (*a*), $CD4^+$ splenic T cells (*b*), and LN cells (*c*) from naive mice (■) and the CIA mice treated with control IgG (○ and ■) or anti-B7h mAb (● and ▨) at day 5 were cultured in the presence or absence of the indicated amounts of dCII for 72 h. In the culture of $CD4^+$ T cells, the mitomycin C-treated immunized splenocytes were added as APCs. Cultures were pulsed with [^{3}H]thymidine and the incorporated radioactivity was measured. *B*, The supernatants of LN cells after a 96-h culture were assessed for IFN-γ and IL-10 production by ELISA. *C*, LN cells from the CIA mice treated with control IgG (■) or anti-B7h mAb (▨) at 10 wk after the secondary immunization were cultured, and proliferation and cytokine production were measured as described above. IL-4 and IL-10 production were undetectable in this culture condition (data not shown). All data are shown as the mean ± SEM of four mice in each group. Data are representative of three independent experiments with similar results. *, Statistically different ($p < 0.05$).

or Th2 cells. Since the anti-CII Abs have been implicated in the pathogenesis of CIA (28), the reduced production of anti-CII Abs might also be responsible for the ameliorating effect of the anti-B7h mAb treatment.

Discussion

In this study, we demonstrated the involvement of the ICOS-B7h costimulatory pathway in the pathogenesis of an experimental murine autoimmune arthritis. The administration of anti-B7h mAb ameliorated the clinical and histological manifestations of CIA. A similar beneficial effect was also obtained by a delayed treatment after the onset of arthritis. Expression of proinflammatory cytokines in the joints and both cellular and humoral responses to CII were significantly inhibited by the anti-B7h mAb treatment, which appeared to result in a beneficial effect.

Various costimulatory molecules, including CD28-CD80/CD86 (6), CD40-CD40 ligand (L) (40), and CD134-CD134L (41), have been implicated in the pathogenesis of CIA. Blockade of the CD28 costimulatory pathway inhibited the development of CIA in mice and rats (6, 42) and CD28-deficient mice were highly resistant to CIA (43), suggesting a critical involvement of CD28 in the induction of CIA. Unlike the constitutive expression of CD28 on naive T cells, ICOS is not expressed on naive T cells but induced after activation (7, 18, 27). In contrast, a considerable level of B7h is expressed on B cells without stimulation (12, 13, 15), whereas CD80 and CD86 are induced by stimulation. Consistent with these reports, we observed a constitutive expression of B7h on B cells in the LNs and the increased number of $ICOS^+$ T cells in the LNs after immunization. In addition to these observations, we first demonstrated the expression of ICOS on T cells and B7h on B cells, macrophages, and dendritic cells in the inflamed joints at protein levels and the increased mRNA expression in the CIA mice. Although further studies are required for the detection of B7h expression on other types of cells in the synovium, our results suggest the possible involvement of ICOS-B7h interactions at the site of joints as well as in the draining LNs.

The actual involvement of the ICOS-B7h interaction in the pathogenesis of CIA was verified by the administration of neutralizing anti-B7h mAb. Blockade of the ICOS costimulatory pathway by anti-B7h mAb resulted in amelioration of inflammatory arthritis as assessed by clinical scoring and histological and radiological examinations. However, this treatment failed to decrease the incidence of disease, while similar treatment with CTLA-4Ig (6), anti-CD154 mAb (40), or anti-CD134L mAb (41) substantially decreased the incidence. Nevertheless, it should be noted that the delayed short-term treatment with anti-B7h mAb was also effective for preventing the progression of disease. In contrast, the treatment with anti-CD4 mAb (44), anti-CD134L mAb (41), or anti-CD80 and CD86 mAbs (6) was not or was less effective after the arthritis had been initiated. These results are consistent with the recent observations in EAE and allergic airway inflammation models, where the blockade of ICOS at the peak of disease, but not during Ag priming, dramatically ameliorated ongoing inflammatory responses (26, 27). Since ICOS is not expressed on naive T cells, it